Chemical Geology 360–361 (2013) 204–219

Contents lists available at ScienceDirect

Chemical Geology

journal homepage: www.elsevier.com/locate/chemgeo

Melt–peridotite reactions in upwelling eclogite bodies: Constraints from EM1-type alkaline basalts in Payenia, Argentina

Nina Søager *, Paul Martin Holm

University of Copenhagen, Department of Geosciences and Natural Resource Management, Øster Voldgade 10, Copenhagen DK-1350 Copenhagen, Denmark

ARTICLE INFO

Article history:
Received 30 November 2012
Received in revised form 17 October 2013
Accepted 18 October 2013
Available online 30 October 2013

Editor: L. Reisberg

Keywords:
Intraplate basalts
Pyroxenite melting
Isotopes
Enriched mantle 1

ABSTRACT

The processes of magma generation in upwelling eclogite bodies of recycled lithospheric material are not fully understood but are important for our understanding and modelling of major and trace element variations in many ocean island basalts (OIB). The primitive alkaline intraplate basalts from the Payenia volcanic province (34–38 °S) in Argentina, for which Sr, Nd and double-spike Pb isotope ratios are presented, and from other north Patagonian volcanic fields may provide details of the eclogite melt–peridotite reactions taking place in the melting column of an upwelling OIB-type mantle. The isotopic composition of the uncontaminated lavas is highly restricted but the Payenia basalts fall in two distinct trace element groups termed the high and low Nb/U groups, which both have EM1-type trace element patterns but with subtle differences that cannot be explained by contamination, fractionation or simple variations in degrees of mantle melting. The difference is also clear in major elements where the low Nb/U basalts have markedly higher alkali contents but lower FeO and Ni than the high Nb/U basalts. Four melt components have been identified based on olivine fractionation corrected compositions: a low Nb/U pyroxenite melt component which is interpreted as an eclogite melt that experienced low degrees of melt–peridotite interaction, a high Nb/U pyroxenite melt component which is interpreted as an eclogite melt that experienced high degrees of melt–peridotite interaction, a low pressure peridotite melt component which contributes to most high Nb/U, Payún Matrú, Matancilla and Auca Mahuida basalts and finally, a melt component with similarities to peridotite melts contributing to many low Nb/U lavas. The high Nb/U type basalts are interpreted to have been formed from mantle with higher temperature than ambient mantle while the low Nb/U basalts may have been formed from normal temperature mantle.

1. Introduction

Basalts erupted in the northern part of the Payenia volcanic province, Argentina, were mainly formed from a South Atlantic MORB-like mantle by addition of fluids from the subducting Nazca slab (Søager et al., 2013). In contrast, the basalts from the southern Payenia province show little evidence for addition of subducted fluids and their isotopes and trace element patterns are typical of EM1 (Zindler and Hart, 1986) ocean island basalts (OIBs) (Kay et al., 2013; Søager et al., 2013). EM1 basalts also occur in Patagonian basaltic provinces further south, for example in the lavas from the north-western Patagonia (Massaferro et al., 2006; Varekamp et al., 2010) and in the Somuncura province (Kay et al., 2007) and in the South Atlantic region, both at hotspots and along the mid-ocean ridge (e.g. le Roex, 1985; le Roex et al., 1990; Douglass and Schilling, 1999; Kamenetsky et al., 2001; Gibson et al., 2005; Willbold and Stracke, 2006; Meyzen et al., 2007; Regelous et al., 2009), suggesting that a specific type of recycled crustal material is frequently present in this mantle region. Willbold and Stracke (2006, 2010) argued that EM1 mantle sources consist of a mixture of recycled oceanic crust and lower continental crust. This is consistent with many isotopic studies (e.g. Kamenetsky et al., 2001; Hanan et al., 2004; Escrig et al., 2005; Meyzen et al., 2005) but is still debated. The aim of this paper is to study the variations in the composition of the EM1 basalts from Payenia to obtain a better understanding of their origin and mode of formation.

Jackson and Dasgupta (2008) linked the EM1 isotopic signature to major element characteristics such as high SiO_2 and very low CaO and CaO/Al_2O_3 suggesting pyroxenitic source lithologies for these basalts. However, the alkalic nature of most EM1 basalts rule out unmodified melts of MORB-like eclogite as primary magmas since such melts are silica-saturated (e.g. Yaxley and Green, 1998; Pertermann and Hirschmann, 2003; Spandler et al., 2008). The experimental studies by Yaxley and Green (1998) and Mallik and Dasgupta (2012) showed that melt–rock reactions between eclogite melt and peridotite can produce alkaline basalts similar to EM1 OIBs, and therefore EM1 sources may contain recycled oceanic crust in the form of eclogite. This is consistent with the work of Wang and Gaetani (2008) who found that the high Ni of pyroxenite-derived basalts, for example from Hawaii (Sobolev et al., 2005, 2007), can in part be generated by equilibration of eclogite melts with mantle olivine which increases the Ni-content of the eclogite melts. Magmas formed from eclogite bodies upwelling

* Corresponding author. Tel.: +45 35322467; fax: +45 35322501.
E-mail address: ns@geo.ku.dk (N. Søager).

0009-2541/$ – see front matter © 2013 Elsevier B.V. All rights reserved.
http://dx.doi.org/10.1016/j.chemgeo.2013.10.024

in normal or low temperature mantle could possibly contain eclogite melts with lower degrees of peridotite interaction than magmas from larger hotspots with higher mantle temperatures. Such melts could provide information about the early phases of melt formation in upwelling eclogite bodies, information which is often obscured by continued melting and melt–rock reactions in hotter mantle. More pristine eclogite melts would be expected to have low Ni, FeO, MgO and CaO and high SiO_2-contents and this type of melt may be present in some of the magmas erupted in northern Patagonia and the Payenia volcanic province. Here, we will show that there is evidence for the contribution from both pyroxenite (possibly eclogite) and peridotite melts in the Payenia and north Patagonian basalts and that a proposed difference in mantle temperature for different volcanic areas may be responsible for the formation of two lava types from the same mantle source with distinctly different major and trace element contents.

2. Geological setting

The Payenia volcanic province is situated in Argentina at ~34–38 °S in the backarc of the Andes Transitional Southern Volcanic Zone (TSVZ) (Fig. 1). The Nazca plate is subducted beneath the area at an angle ~30° and at a speed of ~6.3 cm/a (Kendrick et al., 2003). The province covers more than 40,000 km^2 and includes more than 800 eruptive centres, of which most are basaltic monogenetic or smaller polygenetic centres, but a few large stratovolcanoes such as the late Pleistocene to Recent Payún Matrú volcano also occur.

Volcanism began in the early Miocene with eruption of the OIB-like Matancilla basalts (Kay and Copeland, 2006; Dyhr et al., 2013a, 2013b) which form a large lava plateau beneath and south of the Payún Matrú volcano. In late Miocene to early Pleistocene times, a shallowing of the subducting Nazca slab led to an eastward expansion of the arc and the

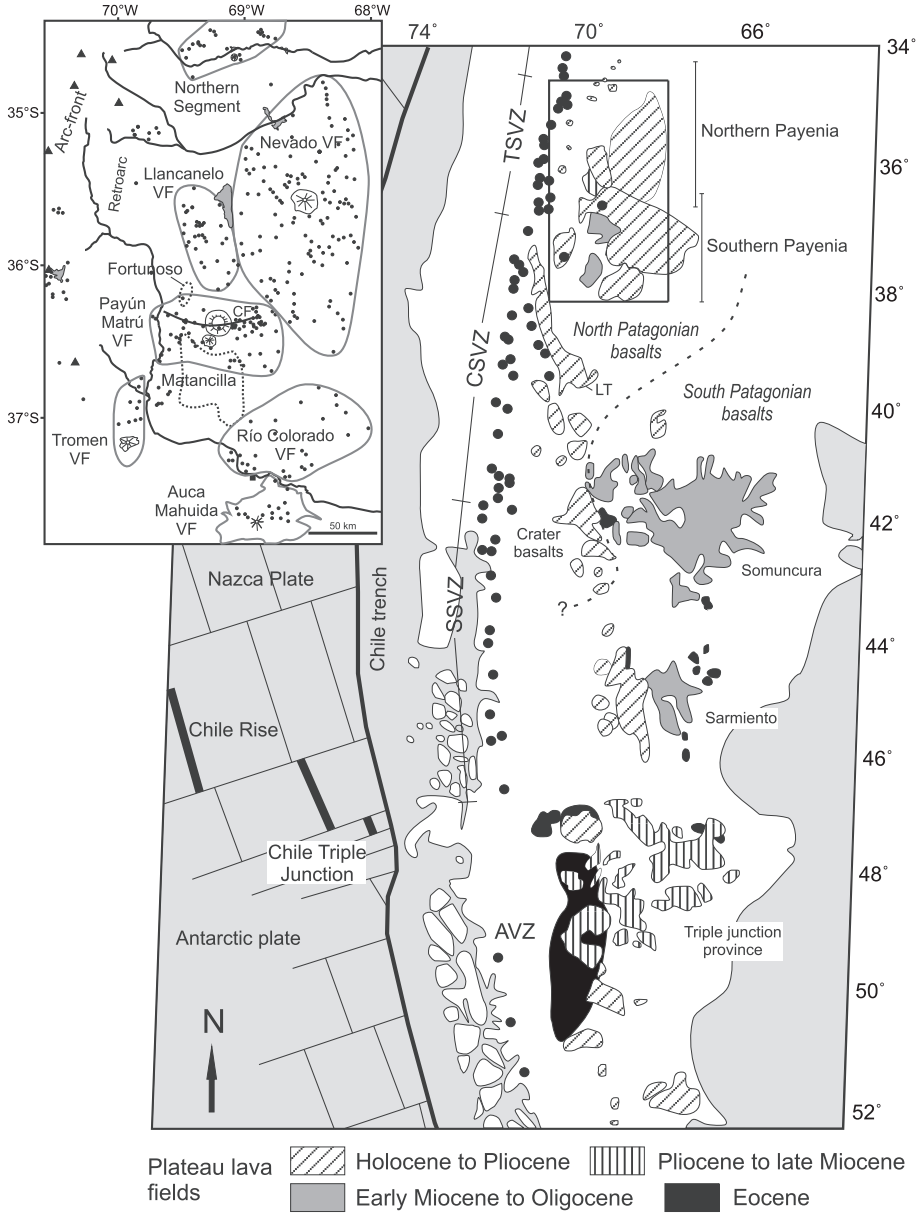

Fig. 1. Map of southernmost South America with the areas of Cenozoic backarc and intraplate volcanism outlined. The square marks the Payenia volcanic province shown in the inset. The black dots mark the young arc volcanoes. The dashed line shows the approximate limit between the occurrence of north and south Patagonian basalts (see Section 5). LT is the Loncopué Trough. TSVZ, CSVZ and SSVZ are the Transitional, Central and Southern Volcanic Zone respectively (after Lopez-Escobar et al., 1995 and Dungan et al., 2001). AVZ is the Austral Volcanic Zone. The map is partly redrawn from Fig. 1 in Kay et al. (2007). The inset is a more detailed map of the Payenia province with the volcanic fields (VF) outlined in grey. The approximate extent of the Early Miocene Matancilla plateau and the Fortunoso cone field is shown with dotted lines. CF is the Carbonilla fracture.

eruption of arc and backarc rocks throughout the Payenia province (e.g. Bermudez et al., 1993; Kay et al., 2006a,b; Litvak et al., 2008; Bertotto et al., 2009; Kay et al., 2013; Søager et al., 2013). Folguera et al. (2009) and Gudnason et al. (2012) demonstrated that by the end of the shallow subduction period, the slab fluid induced volcanism progressed from south to north in the Nevado volcanic field from late Pliocene to ~0.8 Ma and thereafter northwest and west to the Northern Segment and retroarc region where it continued until recently. Gudnason et al. (2012) interpreted the progression of volcanism as a response to the downwarping of the shallow slab from south to north and northwest. The Quaternary period of intraplate volcanism began in the southernmost Auca Mahuida volcanic complex, with ages between ~1.8 and 0.9 Ma (Rosello et al., 2002; Kay et al., 2006a) and moved north to the Río Colorado region, where ages range from 1.5 to 0.3 Ma (Bertotto et al., 2006; Kay et al., 2006b; Gudnason et al., 2012). Finally, volcanism proceeded in the Payún Matrú volcanic complex where the main activity probably started between 0.4 and 0.3 Ma ago and continued until historical times (Germa et al., 2010; Gudnason et al., 2012). However, within the same period there were regular eruptions of large plateau lavas from the eastern part of the Payún Matrú volcanic field from the late Pliocene to late Pleistocene times (Núñez, 1976; Melchor and Casadío, 1999; Dyhr et al., 2013a). Almost all eruptions in the Payun Matrú volcanic field took place along a ~70 km long fracture zone called the Carbonilla fault where the large central volcano is also located. The activity in the Río Colorado region mainly occurred as scattered monogenetic events whereas the Auca Mahuida and Payún Matrú volcanism was of higher intensity with eruption of plateau flows up to 180 km in length (Pasquaré et al., 2008).

3. Previous results

The volcanic rocks from the southern Payenia province are mainly alkaline basalts and trachy-basalts with Mg-numbers (Mg#) between ~45 and 70. More evolved compositions such as trachyandesites and trachytes are mainly found in the Payún Matrú and Payún Liso stratocones and in the Auca Mahuida volcanic complex (Kay et al., 2006a; Germa et al., 2010; Hernando et al., 2012; Kay et al., 2013; Søager et al., 2013). A few trachyandesites are also found among the Matancilla lavas (Kay and Copeland, 2006; Dyhr et al., 2013a).

On the basis of trace element variations, Søager et al. (2013) suggested that the basalts from the Nevado volcanic field and Northern Segment in the northern Payenia province were formed by melting of a MORB-like asthenosphere due to addition of fluids or melts from the subducting slab while the basalts from the Río Colorado (RC) volcanic field in the southernmost Payenia showed no evidence for slab contributions to the melts. Instead these lavas had trace element patterns similar to those of EM1 OIBs. The samples from Auca Mahuida and the Payún Matrú complex in the southern Payenia province have elevated Th/Nb and Ba/Nb and lower Nb/U, Ce/Pb and U/Pb than many RC basalts and this was proposed by Kay et al. (2013) and Søager et al. (2013) to be either due to small amounts of slab fluids in the source mantle and/or to low degrees of crustal contamination.

This paper will give a more detailed description of the published major and trace element variations of the southern Payenia basalts (Río Colorado, Payún Matrú, Auca Mahuida and Matancilla) along with samples from the northwest Patagonian backarc, here called north Patagonian basalts (Crater basalts and Loncopué trough, see references in figure caption 2 and 3) (see Section 6). Furthermore, we provide a new dataset of Sr, Nd and Pb-isotopic analyses for samples from the Río Colorado and Payún Matrú volcanic fields.

4. Analytical procedures

Major and trace element data of the samples were published in Søager et al. (2013). For Pb, Nd and Sr isotopic analysis, 600 mg of hand-picked rock chips were leached for 1 h in 6 N HCl at 120 °C and the residue digested in HF + HNO_3. For the Pb-isotopes, samples were run through anion exchange columns twice. The matrix was eluted in HBr and Pb was collected in 8 N HCl. Analyses were performed in static mode on a VG 54–30 MC-TIMS in Department of Geosciences and Natural Resource Management, University of Copenhagen. Pb was measured using the ^{207}Pb–^{204}Pb double spike technique of Baker et al. (2004) and loading and spiking was carried out according to Thirlwall (2000). Measurements of NBS981 Pb standard yielded an average of $^{206}Pb/^{204}Pb = 16.9390 \pm 0.0029$, $^{207}Pb/^{204}Pb = 15.4992 \pm 0.0038$ and $^{208}Pb/^{204}Pb = 36.7234 \pm 0.012$ (2σ, n = 35). Within run uncertainties are 0.004–0.01 (2 SEM) for all three isotope ratios. Total procedural Pb blanks were below 200 pg.

The eluted solution from the Pb-columns was used for separation of Sr and Nd. The samples were loaded onto cation exchange columns and Sr was extracted in 2 M HCl. Subsequently, the REEs were collected in 6 M HCl. Nd was separated from the REE fraction with Eichrom LN resin in 0.3 M HCl. The Sr and Nd isotope analyses were run in dynamic mode on a VG 54-30 MC-TIMS in Department of Geosciences and Natural Resource Management, University of Copenhagen. Sr and Nd isotopes were mass fractionation corrected to $^{86}Sr/^{88}Sr = 0.1194$ and $^{146}Nd/^{144}Nd = 0.7219$ respectively. The isotope results were monitored by the international standard NBS987 for Sr giving $^{87}Sr/^{86}Sr = 0.710241 \pm 0.000019$ (2σ, n = 54) and JNdi for Nd giving $^{143}Nd/^{144}Nd = 0.512096 \pm 0.000016$ (2σ, n = 52). Total procedural blanks were 600 pg for Sr and 20 pg for Nd. See data in Table 1 and in Supplementary Table 1.

5. Results

The Río Colorado and Payún Matrú samples display a restricted range in Sr, Nd and Pb-isotopic ratios. $^{206}Pb/^{204}Pb$ range from 18.308 to 18.432 and shows a positive correlation with $^{208}Pb/^{204}Pb$ (38.160–38.348) and $^{207}Pb/^{204}Pb$ (15.566–15.593) (Fig. 2b and c). The $^{87}Sr/^{86}Sr$ of the RC basalts (0.70354–0.70391) correlate negatively with $^{143}Nd/^{144}Nd$ (0.51280–0.51286) (Fig. 2a) and range to slightly lower $^{87}Sr/^{86}Sr$ than the TSVZ arc rocks. Although the Payún Matrú samples have the same range of Pb-isotopic ratios as the RC basalts they have higher $^{87}Sr/^{86}Sr$ (0.703675–0.704126) and lower $^{143}Nd/^{144}Nd$ (0.512737–0.512832) in Fig. 2a and form a trend from the RC basalts towards lower $^{143}Nd/^{144}Nd$ and higher $^{87}Sr/^{86}Sr$.

In Pb-isotopic space (Fig. 2b and c) the RC and Payún Matrú samples have $^{207}Pb/^{204}Pb$ ratios in between those of Gough and Tristan islands but lower $^{208}Pb/^{204}Pb$ suggesting a lower time-integrated Th/U ratio of the source. The RC and Payún Matrú rocks are isotopically similar to the rocks from Auca Mahuida, Matancilla, the North Patagonian basalts and some of the South Atlantic MORB data. The North Patagonian and Auca Mahuida basalts plot between the RC samples and the TSVZ arc field at higher $^{206}Pb/^{204}Pb$ probably showing the effect of addition of fluids from the subduction zone (Varekamp et al., 2010; Kay et al., 2013). The north Patagonian and southern Payenia basalts have lower $^{208}Pb/^{204}Pb$ for a given $^{206}Pb/^{204}Pb$ than the central and south Patagonian basalts (Figs. 1 and 2c) and are thus isotopically distinct from these as noted by Stern et al. (1990) who also found them to have distinct trace element patterns.

6. Discussion

6.1. Two trace element groups

As can be seen in Figs. 3 and 4, the southern Payenia basalts fall in two groups with distinct trace element patterns. One group has higher Nb/U and Ce/Pb and lower $(La/Sm)_N$, Th/Nb and K_2O/TiO_2 and generally lower contents of the most incompatible elements than the other group but both groups have similarly high U/Pb and low La/Nb. These groups have been called the high and low Nb/U groups. Basalts from both of these groups are found in the Río Colorado region. The Payún Matrú,

Table 1
Isotopic compositions of Río Colorado and Payún Matrú rocks.

Sample no.	Area	Rock type	Latitude °S	Longtitude °W	$^{87}Sr/^{86}Sr$	2σ	$^{143}Nd/^{144}Nd$	2σ	$^{206}Pb/^{204}Pb$	$^{207}Pb/^{204}Pb$	$^{208}Pb/^{204}Pb$
123944	PM	TB	36.6059	68.6230	0.703675	11	0.512832	10	18.406	15.590	38.161
123944	PM	TB							18.403	15.583	38.151
123946	PM	Basalt	36.6952	68.7529	0.704126	8	0.512737	8	18.431	15.589	38.301
126280	PM	Basalt	36.5348	69.6302	0.703776	15	0.512806	8	18.309	15.566	38.197
123917	PM	Basalt	36.3106	69.6670	0.703964	10	0.512772	10	18.391	15.580	38.293
123926	PM	Basalt	36.4042	69.3327	0.703938	27	0.512800	6	18.437	15.589	38.331
126276	PM	BTA	36.5107	69.3419	0.703783	11	0.512802	8	18.346	15.568	38.243
126268	PM	BTA	36.3803	69.2198	0.704077	8	0.512779	11	18.385	15.580	38.278
126179	RC	TB	37.3183	69.0234	0.703612	8	0.512857	9	18.381	15.578	38.288
126180	RC	Basalt	37.3160	69.0313	0.703548	10	0.512810	16	18.427	15.593	38.348
126178	RC	TB	37.3297	68.9907	0.703535	11	0.512839	29	18.343	15.567	38.223
126177	RC	Tephrite	37.3041	68.9761	0.703691	10	0.512840	8	18.381	15.582	38.285
126176	RC	Tephrite	37.3108	68.9757	0.703550	8	0.512845	7	18.347	15.576	38.244
126175	RC	TB	37.3042	69.0184	0.703753	10	0.512817	8	18.383	15.585	38.307
126173	RC	BTA	37.3025	69.0159	0.703708	7	0.512823	7	18.383	15.582	38.301
126230	RC	TB	37.3288	68.9585	0.703616	10	0.512852	8	18.364	15.578	38.260
126171	RC	Basalt	37.3654	69.0162	0.703551	10	0.512852	8	18.390	15.574	38.282
123972	RC	Basalt	37.2394	69.0899	0.703623	8	0.512851	8	18.367	15.584	38.276
126232	RC	TB	37.3948	68.6658	0.703914	10	0.512795	8	18.394	15.583	38.327
126229	RC	Basalt	37.0521	69.1830	0.703785	13	0.512791	6	18.253	15.571	38.214

TB is trachybasalt, BTA is basaltic trachyandesite. 2σ is given as the standard deviation on the last stated digit.

Matancilla and Auca Mahuida basalts plot along with the high Nb/U group whereas the north Patagonian basalts plot in the low Nb/U group. However, some Payún Matrú, Auca Mahuida and north Patagonian samples trend towards the northern Payenia (N.P) samples indicating addition of slab fluids as was also proposed by Varekamp et al. (2010) for the lavas from the Loncopué trough.

In the plot in Fig. 5, it is clear that the two RC groups have the same range of isotopic compositions and this is true for Sr, Nd and Pb-isotopes. This is surprising given the distinct trace element patterns and suggests that both groups are derived from a common mantle source. Moreover, it suggests that the trace element characteristics of the low Nb/U group magmas have not been generated by crustal contamination of an initially high Nb/U-type magma because this would be expected to change the isotopic composition of the melts unless the contaminating rocks had a very similar isotopic composition as the basalts or very low contents of Sr, Nd and Pb. The fact that the high and low Nb/U basalts range to equally low La/Nb and equally high U/Pb argues against a formation of the low Nb/U group by addition of a slab input to a high Nb/U-type mantle because this typically results in increased La/Nb and decreased U/Pb in the formed melts as seen in the northern Payenia basalts (N.P.) and TSVZ rocks (Figs. 3d and 6d). Addition of slab fluids is also expected to shift the isotopic composition towards the composition of the TSVZ arc rocks which is not the case for the low Nb/U basalts. Secondary alteration processes are also unlikely to have generated the two RC groups because mobile elements such as Cs and U correlate with non-mobile elements like Th within each sample group and show only little scatter (see Fig. A1 in Supplementary Material A). The high and low Nb/U groups cannot have been produced solely by different degrees of melting of the same source either because the degree of melting is too large to allow any significant Nb/U or Th/Nb fractionation (Fig. 3a). If the above mentioned effects can be ruled out as explanation for the formation of the two RC trace element groups, this leaves little other possibilities than trace element fractionation by the presence of different residual phases in the source mantle of the low and high Nb/U melts respectively, or other mineralogical effects taking place during melt extraction from the mantle and passage through the lithosphere.

Table 2
Partition coefficients used in fractionation models illustrated in Fig. 8.

	Ni	Cr	Zn	Co	Sc	Hf	Sr	Nd
olivine		0.937′	1.09*	3.07*	0.265′	0.011′	0.018′	0.007′
clinopyroxene	3.24*	7.1″	0.48*	1.06*	1.15+	0.16+	0.095#	0.191+
spinel	10–		4.50¤	5.00–	0.40¤	0.003!		

*From Le Roux et al. (2011), ″ Skulski et al. (1994), ′ Jeffries et al. (1995), # Johnson (1998), ¤ Horn et al. (1994), ! Elkins et al. (2008), + Hill et al. (2011), – Righter et al. (2006).

6.2. Crust and mantle contamination effects

Lower crustal contamination was suggested by Søager et al. (2013) to be commonly occurring in the whole Payenia region and this has probably also affected some RC, Payún Matrú and Matancilla basalts. Lower crustal rocks such as gabbroic cumulates typically have high Ba/Th, variable but often high Nb/U (or low U/Nb), low U/Pb and lower Th/La, La/Nb and K_2O/TiO_2 than average upper crustal rocks (U/Nb = 0.225, Ba/Th = 59, Th/La = 0.34, La/Nb = 2.6 and K_2O/TiO_2 = 4.4) (Rudnick and Gao, 2003) (Figs. 3 and 6). In Fig. 6b and c, the samples with elevated Ba/Nb relative to the main group of samples have highly variable U/Nb and Ba/Th. Of these samples, many Payún Matrú, Auca Mahuida and north Patagonian basalts are shifted towards higher Ba/Nb, La/Nb, Th/La and U/Nb and at rather constant Ba/Th and $^{87}Sr/^{86}Sr$ (and $^{143}Nd/^{144}Nd$, not shown) and they trend towards the northern Payenia backarc basalts. This suggests that their mantle source was enriched by a slab component enriching the melts in Ba, U, La and Th. The RC, Matancilla, and some of the Payún Matrú basalts (mainly the older lavas from the eastern Payún Matrú fracture) form another type of trends towards higher Ba/Th, Ba/Nb and $^{87}Sr/^{86}Sr$ (and lower $^{143}Nd/^{144}Nd$, not shown), slightly higher or constant La/Nb and Th/La and variable but relatively low U/Nb. Except for the four samples with highest Ba/Th, the increase in Ba/Th is not caused by higher Ba contents in the basalts but by a decrease in the Th contents. Also, the increasing Ba/Th is correlated with decreasing La/Sm but there is no correlation with the SiO_2 content. Altogether this suggests assimilation of depleted lower crustal type rocks, either at lithospheric levels or as melting of delaminated lithosphere in the mantle as suggested by Kay et al. (2013). However, the well-defined trace element compositions of the high and low Nb/U groups in the least contaminated samples with Ba/Th < 210 and Ba/Nb < 17 are similar to OIBs but distinct from typical crustal compositions (Rudnick and Gao, 2003) and therefore they are regarded as source features. To avoid the samples most affected by either slab fluid enrichment or lithospheric contamination, only samples with Ba/Th < 210 and Ba/Nb < 17 have been used in the following figures. Nevertheless, it is seen in Fig. 6 that all Payún Matrú basalts except one (123944) have higher Ba/Nb and La/Nb than most RC basalts and even the samples with Ba/Nb < 17

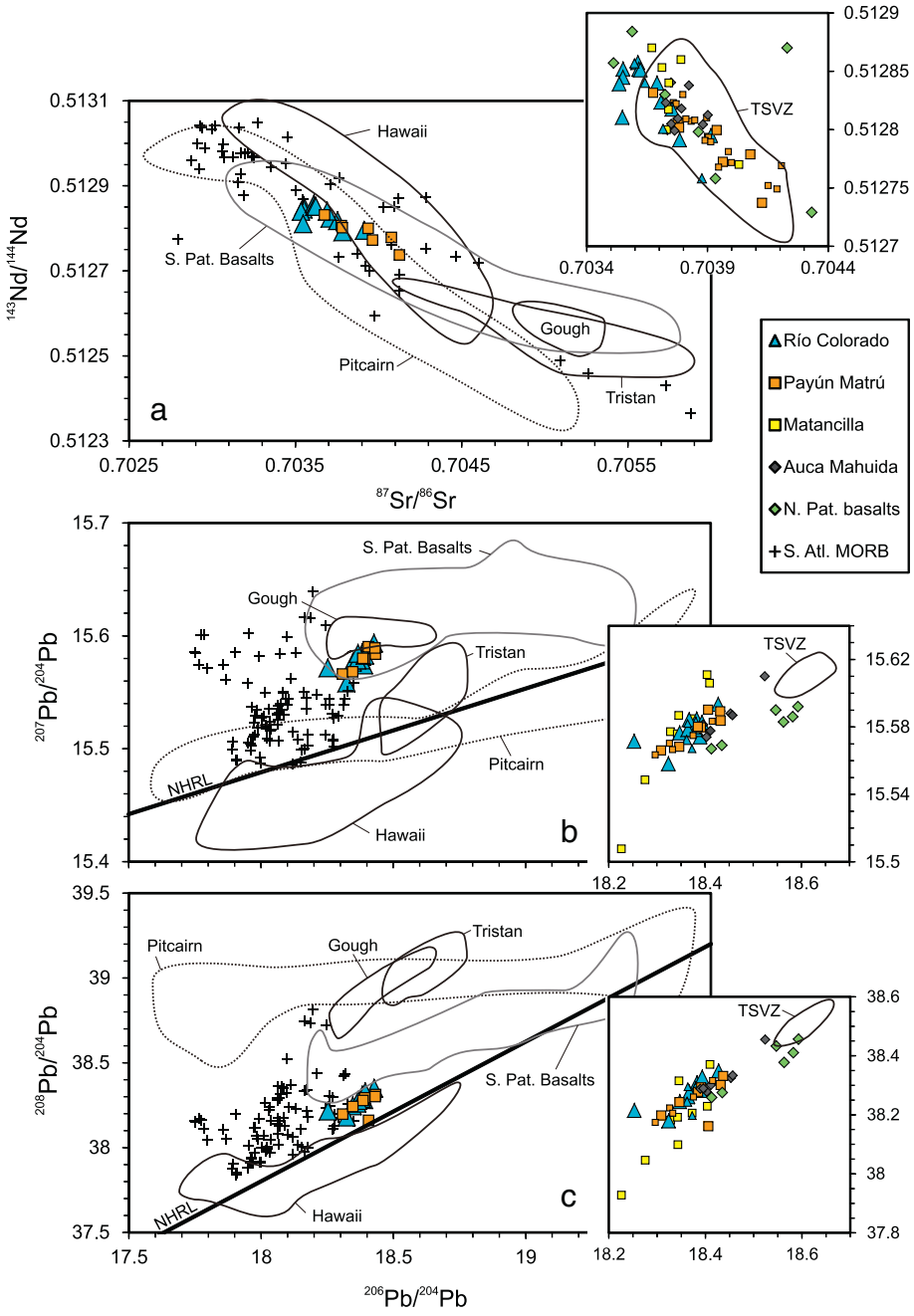

Fig. 2. a) $^{143}Nd/^{144}Nd$ vs. $^{87}Sr/^{86}Sr$, b) $^{207}Pb/^{204}Pb$ vs. $^{206}Pb/^{204}Pb$, c) $^{208}Pb/^{204}Pb$ vs. $^{206}Pb/^{204}Pb$. The large plots show the Río Colorado and Paýun Matrú data from this study along with EM1 OIBs, south Patagonian basalts and south Atlantic MORB. The small inset plots show a close up of the data along with literature data from the Payenia and north Patagonian region and a field for the transitional southern volcanic zone arc rocks (TSVZ). RC and Payún Matrú data from this study have large symbols and literature data have small symbols. The lines in a) and b) are the Northern Hemisphere Reference lines (Hart, 1984). Datasets from Hawaii, Pitcairn, Tristan, Gough and Patagonian basalts are from the GEOROC database (www.georoc.mpch-mainz.gwdg.de) (see references in Supplementary Table A) and from Espinoza et al. (2005), Gorring and Kay (2001), Kay et al. (2004), Kay et al. (2007), Stern et al. (1990), Varekamp et al. (2010). Andes TSVZ: Jacques et al. (2013), Holm et al. (unpublished data). Payún Matrú, Río Colorado and Auca Mahuida: Jacques et al. (2013), Kay et al. (2004, 2013), Pasquaré et al. (2008). Matancilla: Dyhr et al. (2013a, 2013b), Kay and Copeland (2006). South Atlantic (36–47°S) MORB is from www.petdb.org (see references in Supplementary Table A).

therefore probably contain a small slab component. This is probably also the case for most Auca Mahuida basalts as described by Kay et al. (2013).

6.3. A role for lithospheric mantle melts?

Recently, Kay et al. (2013) suggested that the EM1 basalts erupted in the southern Payenia province in the early Miocene and Plio-Pleistocene periods were produced by melting of delaminated lithospheric mantle. Similarly, Jacques et al. (2013) proposed that the Payenia basalts were derived by melting of South American subcontinental lithospheric mantle. The arc and backarc regions are positioned on Proterozoic basement (see summary in Ramos, 2010) and according to Kay et al. (2013), delamination should have taken place here during the whole period and the delaminated material should be the source of the EM1 signature. Unfortunately there is very little xenolith data from this region and the only available data is from the Agua Poca volcano in the Río Colorado volcanic field (Bertotto, 2000, 2003; Conceição et al., 2005). The Agua Poca xenoliths have higher $^{87}Sr/^{86}Sr$ (0.70394–0.70446) and higher $^{143}Nd/^{144}Nd$ (0.51342) than the RC basalts and depleted LREE ($(La/Sm)_N = 0.30$–0.34) which would require exceedingly low degrees of melting (i.e. $\ll 0.01\%$) to generate the high $(La/Sm)_N$ of ~2 in the RC basalts. A feature that these xenoliths share with a large part of other analysed xenoliths

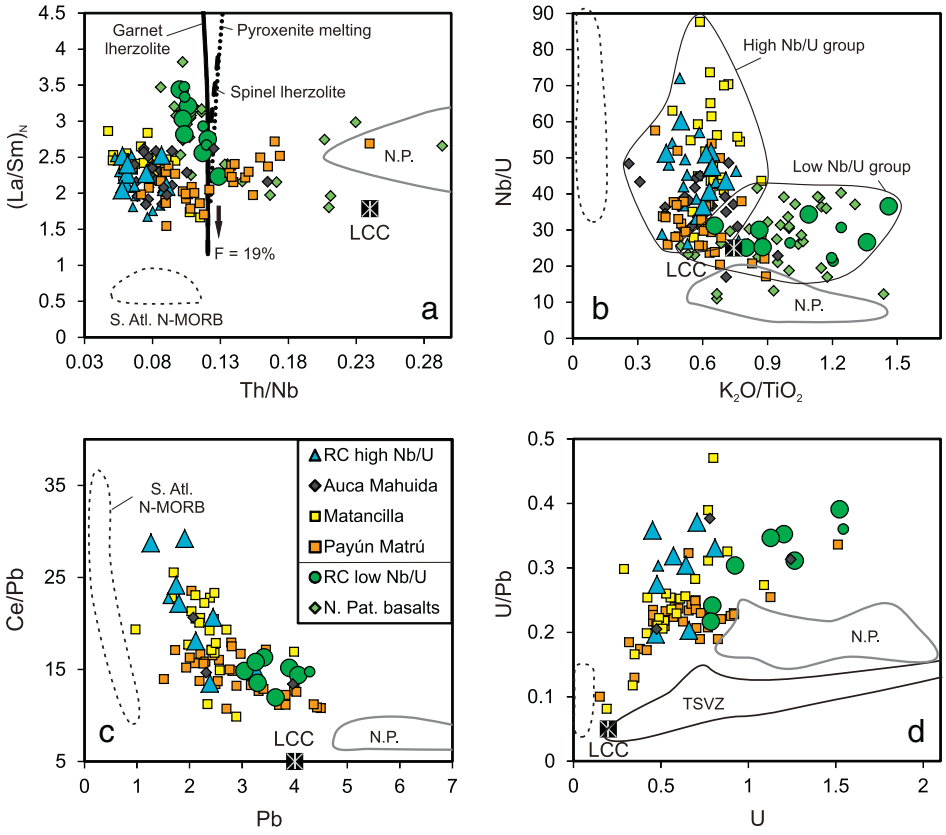

Fig. 3. a) $(La/Sm)_N$ vs. Th/Nb. Normalisation values from McDonough and Sun (1995). b) Nb/U vs. K_2O/TiO_2, c) Ce/Pb vs. Pb, d) U/Pb vs. U. The RC (Río Colorado) samples fall in two groups with high and low Nb/U respectively. N.P. fields show the northern Payenia data from the Nevado volcanic field with Ba/Th < 125 which are regarded as least contaminated (Søager et al., 2013). LCC is the lower continental crust average from Rudnick and Gao (2003). The melting paths in a) show aggregated non-modal batch melting of spinel (dashed line) and garnet (black line) lherzolite with a primitive mantle composition (McDonough and Sun, 1995). Mantle and melting modes are from McKenzie and O'Nions (1995). Distribution coefficients are from Kennedy et al. (1993) (olivine and orthopyroxene), Johnson (1998) (clinopyroxene and garnet), Salters and Longhi (1999) (Th in clinopyroxene and garnet) and Elkins et al. (2008) (spinel). The dotted line shows modal fractional melting of garnet pyroxenite with a primitive mantle composition (McDonough and Sun, 1995) and with modal composition (82% clinopyroxene and 18% garnet) and distribution coefficients from Pertermann et al. (2004). Degree of melting (F) increases with decreasing $(La/Sm)_N$ up to F = 19%. Large RC and Payún Matrú symbols are data from Søager et al. (2013). No literature data from Payún Matrú are shown for clarity. Small RC symbols and Auca Mahuida data are from Bertotto et al. (2009), Jacques et al. (2013) and Kay et al. (2004, 2013). Matancilla: Dyhr et al. (2013a, 2013b). North Patagonian basalts: Massaferro et al. (2006), Muñoz and Stern (1988), Varekamp et al. (2010). TSVZ arc: Jacques et al. (2013). For datasets without Nb measurements, Nb has been calculated as Ta × 18 which is the average Nb/Ta ratio of the RC basalts in the dataset of Søager et al. (2013). Data sources for South Atlantic N-MORB ($(La/Sm)_N < 1$) are the same as in Fig. 2.

from Patagonia (e.g. Conceição et al., 2005; Bjerg et al., 2009; Dantas et al., 2009) and northern Argentina (Lucassen et al., 2005) is the low contents of Ba and Rb relative to Th and U resulting in often very low Ba/Th ratios (Ba/Th = 22 in Agua Poca xenolith from Conceição et al., 2005). Since the Ba/Th ratio is largely unaffected by melting processes except for very low degree melts (F < ~1%) (Stracke and Bourdon, 2009) this type of lithospheric mantle would not be able to generate the RC basalts which all have Ba/Th > 100. If instead the lithospheric mantle fragments were enriched by slab fluids they could be enriched in Ba but then they would also be expected to be enriched in Pb and U and have low Ce/Pb and Nb/U which the RC basalts are not. However, lithospheric mantle xenoliths display a wide variety of trace element compositions and it is difficult to draw unambiguous conclusions on this basis.

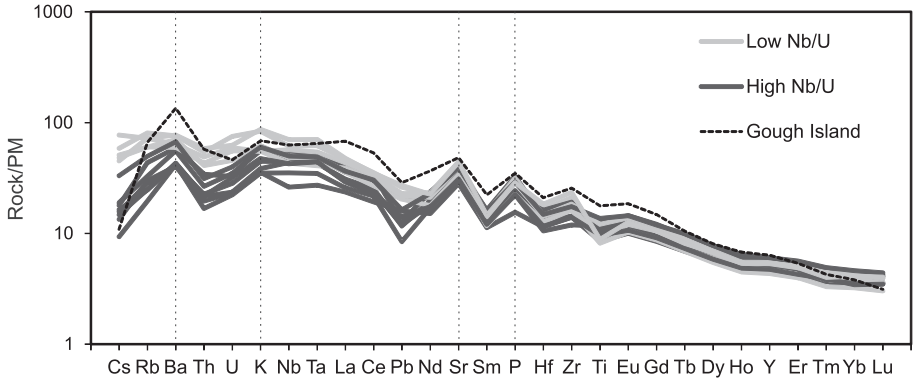

Fig. 4. Primitive mantle-normalised trace element patterns of the high and low Nb/U RC samples from Søager et al. (2013) which show the difference in trace element contents between the two groups. The two low Nb/U samples with Ba/Nb > 17 are not plotted. A sample from Gough Island (G131, Willbold and Stracke, 2006) has been shown for comparison. Normalisation values from McDonough and Sun (1995).

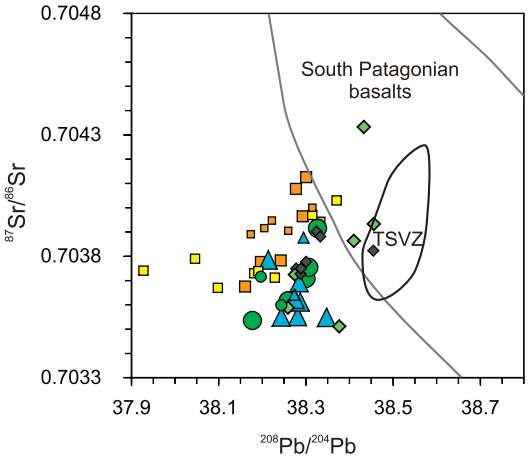

Fig. 5. $^{87}Sr/^{86}Sr$ vs. $^{208}Pb/^{204}Pb$. Legend as in Fig. 3. The RC high and low Nb/U groups have the same range of isotopic compositions and do not trend towards the TSVZ arc field. Some samples from north Patagonia and Auca Mahuida plot close to the arc field indicating incorporation of a slab component into the magmas. Data sources are as in Fig. 2.

Another argument against derivation of the southern Payenia basalts from local delaminated lithospheric mantle is the homogeneity in the isotopic composition of the samples (Fig. 2), the well-defined trace element compositions of the high and low Nb/U groups (Fig. 3) and the fact that these basalt compositions have been erupted in a fairly large area since the early Miocene. Mantle xenoliths are often very heterogeneous both in isotope and trace element space, even within xenoliths from the same volcano (e.g. Lucassen et al., 2005; Bjerg et al., 2009). As an example, the mantle xenoliths from a Cretaceous rift setting in NW Argentina (Lucassen et al., 2005) have age corrected (100 Ma) $^{206}Pb/^{204}Pb$ ranging from 16.43 to 20.59. The host basanites possibly partly derived by melting of this lithosphere have a more restricted range of age corrected (90 Ma) $^{206}Pb/^{204}Pb$ (18.43–19.17) (Lucassen et al., 2002) but still much more variable than the southern Payenia basalts. It thus seems unlikely that the southern Payenia basalts are formed by melting of local lithospheric mantle, whether it is delaminated or in situ. Therefore the Payenia source is regarded as an asthenospheric mantle source and the EM1 signature could be derived from ancient recycled oceanic and continental lithospheric material.

6.4. Recycled crust as a source for the EM1 signature

The trace element patterns of the RC basalts shown in Fig. 4 and the sample from Gough Island (Willbold and Stracke, 2006) all have relatively high contents of Ba, K and Sr relative to Th, U and REE elements such as Nd causing them to have high Sr/Nd and Ba/Th ratios (Fig. 7). The same type of trace element pattern is found in other EM1 basalts such as the Patagonian Somuncura basalts (Kay et al., 2007), the Koolau basalts from Hawaii (e.g. Frey et al., 1994; Ren et al., 2009), Discovery seamount and the South Atlantic LOMU MORB (le Roux et al., 2002; le Roex et al., 2010) and has been proposed to reflect small amounts of lower continental crust along with recycled oceanic crust in the mantle sources (e.g. Willbold and Stracke, 2006; Stracke and Bourdon, 2009; Willbold and Stracke, 2010).

A mixing trend between recycled MORB (Stracke and Bourdon, 2009 and references herein) and average lower continental crust (Rudnick

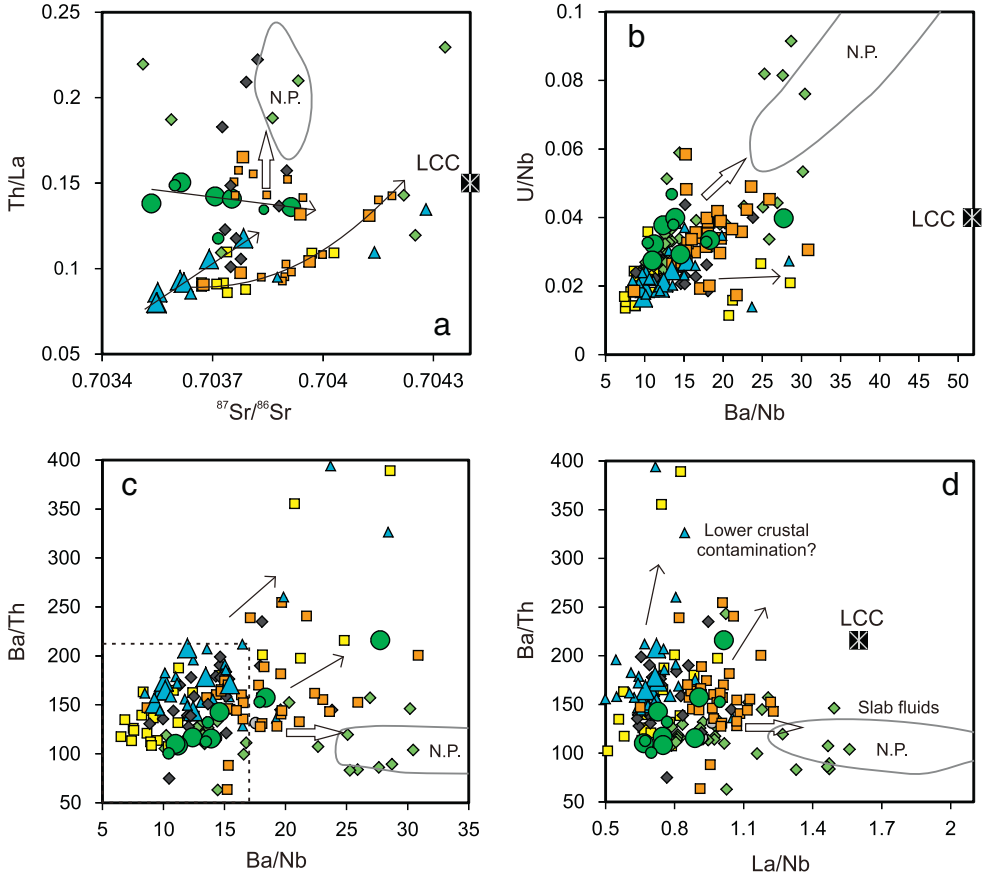

Fig. 6. a) Th/La vs. $^{87}Sr/^{86}Sr$, b) U/Nb vs. Ba/Nb, c) Ba/Th vs. Ba/Nb, d) Ba/Th vs. La/Nb. The white arrows point towards the northern Payenia basalts (N.P.) and show the effect of addition of slab fluids and melts. The thin black arrows outline the trends interpreted to be caused by lower crustal contamination. LCC is the lower continental crust average of Rudnick and Gao (2003). In c) the dashed square encloses the samples identified as least contaminated and least affected by slab fluids. Samples with Ba/Nb > 17 and Ba/Th > 210 will not be used in the following figures.

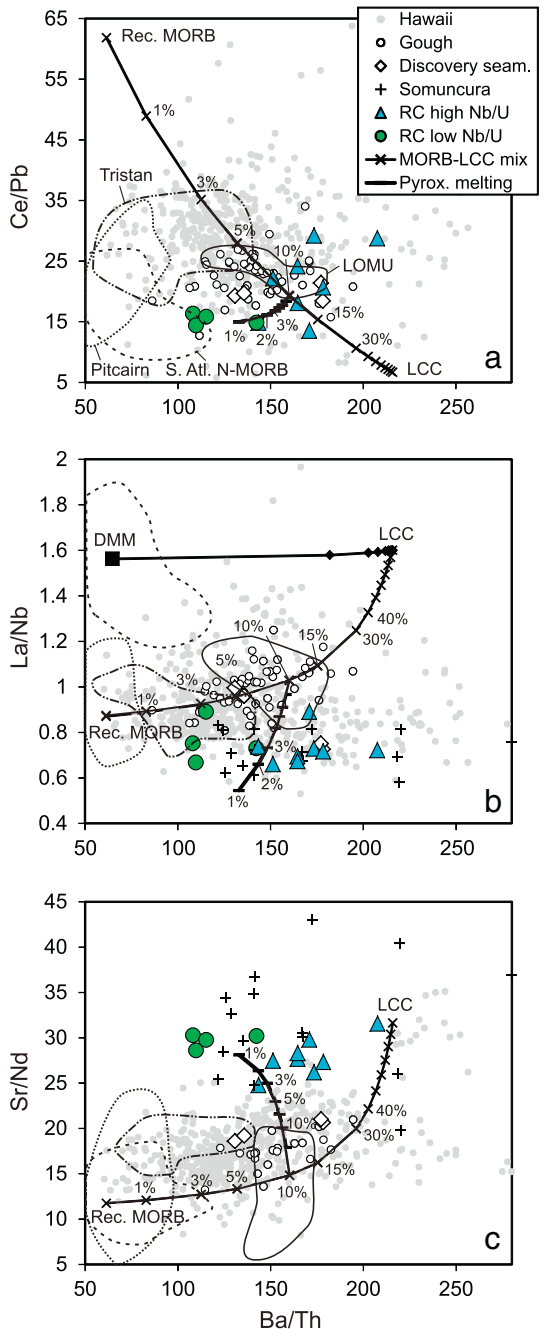

Fig. 7. a) Ce/Pb vs. Ba/Th, b) La/Nb vs. Ba/Th and c) Sr/Nd vs. Ba/Th variations of global EM1 occurrences. Many samples plot close to the mixing trajectory (marked with Xs) between recycled MORB, based on the composition given by Stracke and Bourdon (2009), and average lower continental crust (LCC, Rudnick and Gao, 2003). The Pb content of the LCC has been set to 3 ppm instead of 4 ppm in agreement with Willbold and Stracke (2006) and this causes a better fit of the mixing curve to the data in a). The mixing trajectory in b) marked by black diamonds is made between LCC (Rudnick and Gao, 2003) and depleted mantle (DMM) with concentrations taken from Workman and Hart (2005). Tick marks indicate the percentage LCC in the mixtures. The solid lines marked with horizontal bars illustrate how the plotted ratios are affected by pyroxenite melting of a source containing 90% rec. MORB + 10% LCC. They are based on modal fractional melting of a pyroxenite source with 82% clinopyroxene and 18% garnet using the KDs of Pertermann et al. (2004). Tick marks indicate 1, 2, 3, 5, 7 and 10% melting. The South Atlantic N-MORB field includes samples with $(La/Sm)_N < 1$. Somuncura have not been plotted in a) because there are no data for Pb available. Data sources as in Fig. 2 and for Discovery seamount: le Roex et al. (2010), Somuncura (part of the south Patagonian basalts in Fig. 1): Kay et al. (2007).

and Gao, 2003) is shown in Fig. 7. The model assumes solid state mixing and homogenisation of the sources before melting. Also shown is a pyroxenite melting trajectory. Pyroxenite melting generates the most extreme fractionation of the used ratios during melting while peridotite melting fractionates the ratios considerably less (Stracke and Bourdon, 2009). In particular the Sr/Nd ratio is highly variable during pyroxenite melting and was proposed by Stracke and Bourdon (2009) to be a strong indicator for source pyroxenite and this could explain why most of the EM1 samples plot above the recycled MORB–LCC mixing line in Fig. 7c. In the mixing model, most of the EM1 basalts (including the RC basalts) indicate ~3 to 15% lower continental crust in the mixture which is in accordance with the 10% estimated by Willbold and Stracke (2006). Yet, the difference between the high and low Nb/U groups cannot be explained by higher or lower amounts of LCC in the source because the lower Ba/Th of the low Nb/U group should then have been accompanied by higher Ce/Pb (and Nb/U) which is not the case. Whether the South Atlantic EM1 occurrences are shallowly or deeply recycled material is controversial and there are reasons to believe that both scenarios occur (e.g. Hawkesworth et al., 1986; Fontignie and Schilling, 1996; Milner and le Roex, 1996; Douglass and Schilling, 1999; Kamenetsky et al., 2001; le Roux et al., 2002; Escrig et al., 2005; Gibson et al., 2005; Meyzen et al., 2007; Regelous et al., 2009; Class and le Roex, 2011). The low La/Nb and high U/Pb (not shown) of most of the plotted EM1 basalts require the presence of an equivalent source component, such as recycled MORB, because mixing between depleted mantle (DMM, Salters and Stracke, 2004; Workman and Hart, 2005) and typical upper or lower crustal material would give high La/Nb (Fig. 7b) and low U/Pb. The presence of recycled oceanic crust along with continental crustal material in many South Atlantic and other EM1 sources was also proposed by Willbold and Stracke (2010) based on the isotopic variations. Willbold and Stracke (2010) argued that recycling of oceanic lithosphere and continental crustal fragments in subduction zones is the most likely way of explaining the common occurrence of EM and recycled oceanic crustal components in OIBs. Furthermore, the supply of a geochemically homogeneous OIB-like mantle source to the Payenia region during the last 25 Ma is difficult to reconcile with melting of random rafting fragments of lithosphere, but rather suggests tapping of a larger reservoir of at least locally homogenised subducted crustal material.

6.5. Major element variations in southern Payenia and north Patagonian rocks

The fractionation trends outlined by the sample sequences from the Payún Matrú and Auca Mahuida volcanoes both indicate that plagioclase is not removed from the liquids until ~5 wt.% MgO (Mg# ~55–58) (Kay et al., 2013; Søager et al., 2013). This is also supported by the Sr/Nd variation in all sample groups (Fig. 8c) which show a decreasing Sr/Nd with decreasing Mg# below Mg# ~55–58 suggesting the initiation of plagioclase fractionation at this stage. According to Kay et al. (2013) this is due to fractionation of the mafic magmas at deep crustal levels but the plagioclase fractionation could also be retarded if the magmas contained small amounts of water (1–1.5%) (Søager et al., 2013).

The more mafic samples (Mg# > ~55–60) from southern Payenia and north Patagonia in Fig. 8 have highly variable CaO/Al_2O_3 and Sc/Hf and decreasing Cr and Ni with decreasing Mg# which indicates that olivine and small amounts of chromite were the only fractionating phases at this stage. Below Mg# ~55–60, the CaO/Al_2O_3 and Sc/Hf sharply decreases suggesting that clinopyroxene becomes a major constituent in the fractionating assemblage at this point fractionating along with plagioclase. Due to the high contents of Cr in spinels crystallising from mafic melts (Barnes and Roeder, 2001) (36–24 wt.% Cr_2O_3 in the spinels used for the olivine + spinel fractionation model in Fig. 8) the amount of spinel crystallising along with olivine cannot have been more than 1–1.5% if the trend of the samples should be reproduced (Fig. 8d). This small amount causes almost no difference from the pure olivine

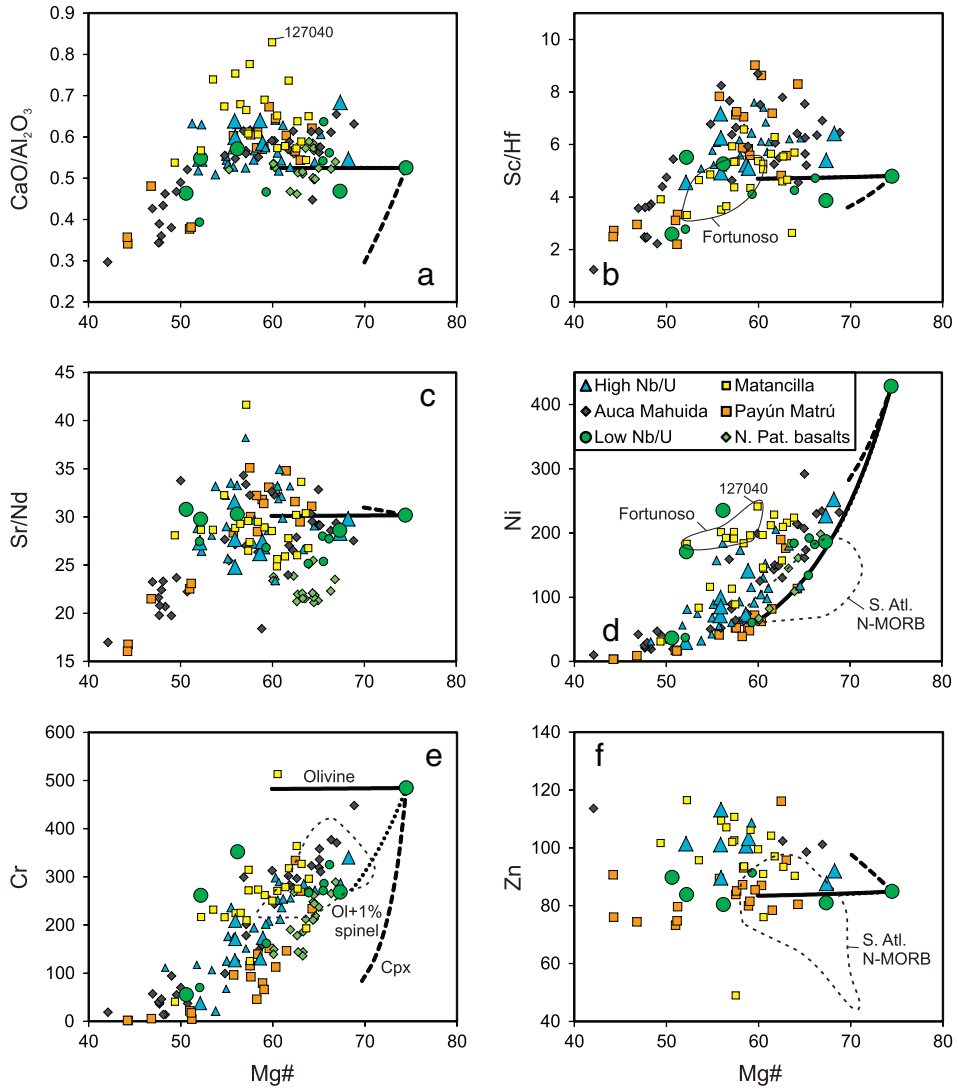

Fig. 8. a–f: Mg# vs. CaO/Al_2O_3, Sc/Hf, Sr/Nd, Ni, Cr and Zn. The Matancilla (Fortunoso) sample 127040 from Dyhr et al. (2013b) is indicated in a) and d) because it has the highest CaO/Al_2O_3 and olivine fractionation corrected Ni (see Fig. 9). The Matancilla samples from the Fortunoso cone field are outlined in b) and d). In a–f), the black lines show the effect of 20% equilibrium olivine fractionation assuming a $Kd^{ol}_{(Fe/Mg)} = 0.3$ and FeO/FeO^T (whole rock) = 0.8. The $Kd^{ol}_{(Ni)}$ has been calculated according to the model of Hart and Davies (1978). The dashed lines show the effect of 25% fractionation of clinopyroxene. The dotted line in e) shows the effect of 10% fractionation of 99% olivine + 1% chromite. In the other plots, the dotted lines are coincidental with the pure olivine fractionation lines. All used distribution coefficients are listed in Table 2. References for south Atlantic N-MORB are as in Fig. 2.

fractionation trends in plots of Ni and Zn vs. Mg# (Fig. 8d and f) and it would have had very little effect on the major and trace element contents of the magmas in general.

In Fig. 8d, a part of the Matancilla basalts form a trend with almost constant Ni at decreasing Mg# (samples outlined in Fig. 8b and d) suggesting a different fractionation path than the other basalts. These samples are from the early Miocene Fortunoso cone field north of Payún Matrú (Dyhr et al., 2013b) and display some of the highest Ni contents for a given Mg# observed. This subgroup has decreasing Sc/Hf but not Sr/Nd with decreasing Mg# and the sub-horizontal trend in Fig. 8d could thus be related to fractionation of higher amounts of clinopyroxene relative to olivine compared to the other groups. However, only the most mafic of these samples (127040) with Mg# = 60 is used for the olivine fractionation correction below (Section 6.5.1). This sample has similar Sc/Hf as other Matancilla basalts with Mg# > 60 and the highest CaO/Al_2O_3 of all samples used and therefore it cannot have fractionated any significant amounts of clinopyroxene. Nevertheless, the fractionation corrected Ni content may deviate from the true Ni content of the mantle melts.

In Fig. 8d to f, most of the RC low Nb/U, north Patagonian and Payún Matrú basalts have low Ni, Cr and Zn (and Co, not shown) for a given Mg# like the south Atlantic N-MORB samples which are presumably mainly derived by peridotite melting. Relative to these, the RC high Nb/U, Auca Mahuida and Matancillla basalts have higher and highly variable contents of Ni, Cr and Zn. The higher concentrations cannot have been caused by accumulation of chromite, in which these minor transition elements are highly compatible, as suggested by Varekamp et al. (2010), because addition of sufficient chromite to increase the Ni and Zn to the levels of for example the Matancilla basalts would increase the Cr contents to wt.% levels which is not seen. Likewise, early fractionation of clinopyroxene is not able to explain the higher concentrations of Ni, Cr and Zn in the RC high Nb/U, Auca Mahuida and Matancillla basalts because the high Nb/U basalts should then have had lower Cr, Sc/Hf and CaO/Al_2O_3 than the low Nb/U basalts since Cr, Sc and CaO are compatible in clinopyroxene, and this is not the case. In the same way, the lower Cr and low CaO/Al_2O_3 of many low Nb/U basalts cannot have been caused by early fractionation of clinopyroxene because they should then have higher Ni and Zn than the high Nb/U basalts. The higher Ni, Cr and Zn contents of the high Nb/U, Auca Mahuida and Matancilla basalts therefore appear to be a feature inherited from the primitive melts. The fact that these minor transition elements are more compatible in olivine and spinel than in other mantle minerals

could suggest that one or both of these minerals were somehow responsible for the increased concentrations.

6.5.1. Peridotite and pyroxenite melting in the Payenia source mantle

In order to approach the primitive melt compositions, the samples with Mg# > 60 have been olivine fractionation corrected to equilibrium with Fo_{88} olivine (Mg# 68.8) (Fig. 9). This Mg# was chosen based on the observed range of Mg-numbers in the data and micro-probe analyses of olivines in sample 126175, yielding $Fo_{86–87}$ as maximum Fo-contents (F.E. Brandt, pers. comm.). The correction was made by addition or subtraction of equilibrium olivine in steps of 0.1% assuming a $Kd^{ol}_{(Fe/Mg)} = 0.3$ and FeO/FeO^T (whole rock) = 0.8 until Mg# = 68.8 was reached. Ni was corrected according to the olivine partition coefficient model of Hart and Davies (1978). Results can be found in Supplementary Table B.

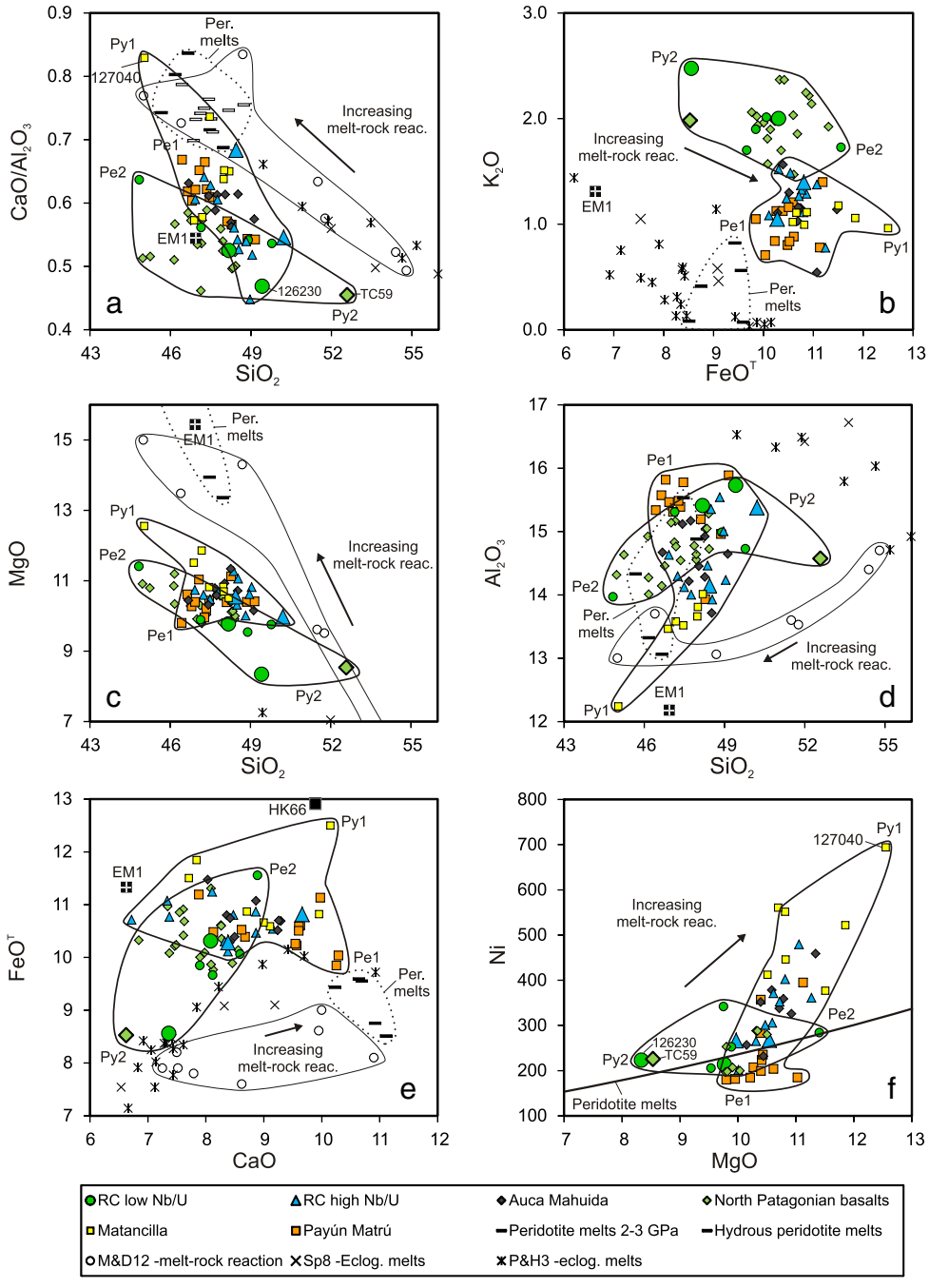

Fig. 9. Olivine fractionation corrected major element compositions of Payenia and North Patagonian basalts. Large RC symbols are data from this study. a) CaO/Al_2O_3 vs. SiO_2, b) K_2O vs. FeO^T c) MgO vs. SiO_2, d) Al_2O_3 vs. SiO_2 e) FeO^T vs. CaO. Samples 126230 and TC59 (Muñoz and Stern, 1988) show the closest resemblance to eclogite melts. HK66 is a melt composition (3 GPa) from highly fertile peridotite (Hirose and Kushiro, 1993). The data from Mallik and Dasgupta (2012) shows the effect of progressive melt–rock reaction between an eclogite melt and peridotite. The EM1 composition is the average composition of primitive Pitcairn Island basalts from Jackson and Dasgupta (2008) which represent global EM1 OIBs. Py1 and Py2 are presumably pyroxenite-derived melt components and Pe1 and Pe2 are peridotite-like melt components (see text for explanation). f) Ni vs. MgO. The line shows calculated melt compositions in equilibrium with peridotite (after Herzberg, 2011). The Crater basalts from Massaferro et al. (2006) (part of the N. Pat. basalts) analysed at Actlabs have been left out of f) because they have significantly lower Ni concentrations at a given Mg# than the samples analysed at the University of Pisa (also from Massaferro et al., 2006) and all other samples plotted in Fig. 9. Data sources as in Figs. 2 and 3 and fertile peridotite melts (F = 12.6–16.6): Hirose and Kushiro (1993) (KLB-1), Walter (1998) (KR4003), hydrous peridotite melts (3 GPa): Balta et al. (2011), eclogite melts: Pertermann and Hirschmann (2003) (P&H3), Spandler et al. (2008) (Sp8).

The corrected analyses display a considerable span in compositions with CaO ranging from 10 down to only 7 wt.% suggesting melt contributions from both peridotite and other mantle lithologies. The samples with the highest CaO and lowest K_2O contents (Fig. 9a and e) approach melts of experimental fertile peridotite. In particular, many Payún Matrú basalts have high CaO and CaO/Al_2O_3 and low Ni suggesting that they have an important peridotite melt component (termed the Pe1 component). Further olivine fractionation correction, for example to equilibrium with Fo_{90} olivine, would only have a small effect on the SiO_2, CaO, FeO^T and Al_2O_3 but it would raise the MgO from around 10 to 12 wt.% in the Payún Matrú basalts causing them to be more similar to the experimental peridotite melts in this aspect. The low MgO content of ~10 wt.% of the Pe1 melt component may be related to a relatively low degree of melting and/or a low pressure during the peridotite melting (e.g. Hirschmann et al., 1999; Herzberg and Asimov, 2008).

The RC, Auca Mahuida and North Patagonian basalts have lower CaO and CaO/Al_2O_3 than the experimental peridotite melts. The low Nb/U sample 126230 and the North Patagonian sample TC59 (Muñoz and Stern, 1988) have the most extreme compositions with low CaO (7.4 and 6.7 wt.% respectively), FeO^T (8.6 and 8.5 wt.%), MgO (8.3 and 8.2 wt.%) and Ni (222 and 206 ppm) but relatively high SiO_2 (49.4 and 52.7 wt.%) and high K_2O (2.47 and 2.0 wt.%). These compositions are similar to high-degree eclogite melts (e.g. Yaxley and Green, 1998; Pertermann and Hirschmann, 2003; Spandler et al., 2008) (Fig. 9). However, they have far lower CaO and CaO/Al_2O_3 than both anhydrous and hydrous peridotite melts (e.g. Hirose and Kushiro, 1993; Gaetani and Grove, 1998; Walter, 1998; Balta et al., 2011). This observed eclogite-like melt composition has been termed the Py2 melt component. The K_2O content of the Py2 component is much higher than in the basaltic melts from the eclogites investigated experimentally (Fig. 9b) so if the Py2 component represents high degree eclogite melts it must have been a highly K-rich eclogite. The K-enrichment could instead be related to incorporation of continental lithospheric material, such as lower crust, into the mantle source. The very low CaO/Al_2O_3 and high SiO_2, K_2O and K_2O/TiO_2 (up to 1.46) of the Py2 component is characteristic for EM1 basalts (Jackson and Dasgupta, 2008) and has been proposed to reflect melting of recycled oceanic and continental crust in the form of eclogite (e.g. Yasuda et al., 1994; Pertermann and Hirschmann, 2003; Sobolev et al., 2005; Herzberg, 2006; Sobolev et al., 2007; Spandler et al., 2008; Herzberg, 2011; Mallik and Dasgupta, 2012).

6.5.2. Peridotite equilibration of eclogite melts

The combination of relatively low Ni and low CaO in the Py2 component is different from what is seen in many hotspot lavas that are related to pyroxenite melting (e.g. Sobolev et al., 2005, 2007; Herzberg, 2011) and this melt component may represent eclogite partial melts which are expected to have low Ni contents (Sobolev et al., 2005; Wang and Gaetani, 2008). By contrast, the intermediate CaO and high Ni contents of many of the Auca Mahuida and RC high Nb/U samples, and in particular the Matancilla basalts, define another melt component termed the Py1 melt component (Fig. 9f). The high Ni of the Py1 component suggests the operation of similar processes as in hotspots like Hawaii and the Canaries where high Ni olivines and lavas are common in pyroxenite derived basalts (Sobolev et al., 2005, 2007; Gurenko et al., 2009, 2010; Herzberg, 2011). With the high CaO-low Ni Pe1 peridotite melt-like component, major element variations therefore suggest involvement of at least three different melt components: Pe1, Py1and Py2. The melt components represent different major element melt compositions which, however, are not necessarily derived from different mantle sources. Rather, the homogeneous isotopic compositions of these samples suggest derivation from a common heterogeneous mantle source, which became heterogeneous recently.

In detail, a fourth melt component termed Pe2 is necessary to explain the variation of the low Nb/U basalts which show a considerable range of in particular SiO_2 and FeO^T. Mixing of Py2 with Pe2 melts leads to increasing MgO, FeO^T, and CaO/Al_2O_3 and decreasing SiO_2 and Al_2O_3 but at similarly low Ni and high alkali contents. These characteristics suggest that the Pe2 component could be peridotite melt-like. The rather low SiO_2-content of many RC low Nb/U and North Patagonian samples relative to the high Nb/U samples seems to be caused by mixing with this low silica Pe2 component that apparently contributed to many of these melts. The low Al_2O_3 and SiO_2 and high alkali content suggest that Pe2 could represent peridotite melts formed at deep levels and at very low degrees of melting (see for example Herzberg and Asimov, 2008) but it would have to be a highly Fe-rich low Mg# peridotite such as the HK66 fertile peridotite composition used in the melting experiments of Hirose and Kushiro (1993) to yield the high FeO^T-contents (Fig. 9e). Alternatively they could be derived from a silica-undersaturated pyroxenite source since these typically produce melts very similar to peridotite melts (see Herzberg (2011) and Kogiso et al. (2004) and references herein) or they could reflect small amounts of olivine in some parts of the eclogite source which would cause formation of silica-undersaturated melts due to a change in the melting phase relations (Kogiso et al., 1998, 2004).

The Pe1 peridotite melt component dominates the Payún Matrú basalts, but also appears to have contributed to many of the RC high Nb/U, Matancilla and Auca Mahuida basalts. The high Al_2O_3 contents of the Payún Matrú samples (Fig. 9d) are similar to experimental peridotite melts formed at 2–2.5 GPa (Hirose and Kushiro, 1993) and suggest that they have been formed at relatively low pressures. The Py1 melt component has high Ni, FeO^T, MgO and CaO/Al_2O_3, intermediate CaO and low SiO_2, Al_2O_3 and alkali contents and is represented by the Matancilla basalts which have the highest fractionation corrected Ni concentrations (Fig. 9f). This melt component apparently plays an important role in the formation of the RC high Nb/U and Auca Mahuida basalts. The Py2 pyroxenite component is most important in the RC low Nb/U and North Patagonian basalts but also part of the RC high Nb/U and Auca Mahuida basalts are shifted in the direction of the Py2 component at higher SiO_2 and lower CaO/Al_2O_3 than the Pe1 and Py1 components (Fig. 9a) and therefore Py2 melts apparently also played a role in the formation of the high Nb/U type magmas. In summary, the RC low Nb/U and North Patagonian basalts have apparently been formed by mixing between the Py2 and Pe2 melt components whereas the RC high Nb/U, Auca Mahuida and Matancilla basalts indicate mixing between primarily the Py1 and Pe1 melt components with a minor role for the Py2 component. These melt components have some similarities to the melt components defined by Dasgupta et al. (2010) for a dataset of global OIB. These authors found that, apart from contributions from low pressure peridotite melts in basalts from ridge-near hotspots, the OIBs plotted between a low SiO_2–high FeO^T component (similar to the Py1 component from this study but with a more extreme composition and interpreted to be derived from carbonated eclogite) and a high SiO_2–high FeO^T component with somewhat lower FeO^T. The high SiO_2–high FeO^T component is somewhat similar to the Py2 component from this study and was also interpreted to represent silica-excess pyroxenite melts. The major element compositions of the southern Payenia and North Patagonian basalts therefore seem to reflect processes which are also operating in global OIB formation.

Sobolev et al. (2005, 2007) suggested that the Hawaiian high Ni picritic basalts were generated from garnet websterite formed by the reaction between eclogite melts and peridotite. However, the recent study of Mallik and Dasgupta (2012) showed that the amount of melt before and after the reaction between eclogite melt and peridotite is the same. This eliminates the need for a solid second stage pyroxenite and the basaltic melts may simply be formed by reaction between eclogite melts and peridotite during ascent in the magma conduits.

In the experiments of Mallik and Dasgupta (2012) and Yaxley and Green (1998) the reaction between andesitic eclogite melts and peridotite caused consumption of olivine in particular but also clinopyroxene and garnet in the peridotite and precipitation of orthopyroxene. This increases the MgO, CaO and FeO^T and decreases the SiO_2, Al_2O_3, Na_2O and K_2O in the eclogite melt as the melt–rock reaction proceeds (Fig. 9c, d, e

and f) (Mallik and Dasgupta, 2012). Wang and Gaetani (2008) showed that also Ni increases in the melt when eclogite melts equilibrate with olivine. The result is a transition from silica-saturated low Mg#-low Ni andesitic melts to silica-undersaturated higher Mg#-high Ni basaltic melts. The major element variation from Py2 to Py1 melts could reflect an increasing degree of melt–rock interaction between eclogite melt and peridotite generating major element trends similar to the experimental melts of Mallik and Dasgupta (2012) and increasing the Ni concentrations of the melts. The reacted melts subsequently mix to various extents with Pe1 peridotite melts formed at lower pressures. The high Ni content of the Py1 melt component (560–700 ppm) is comparable to those of the Koolau lavas (~700–900 ppm, Sobolev et al., 2005). However, the Ni contents are highly dependent on the degree of fractionation correction and increase significantly if the samples are fractionation corrected to equilibrium with Fo_{90}, so the true fractionation corrected Ni concentrations depend on the Mg# of the real primary liquids.

The large difference in FeO^T between the Py1 and Py2 components is not reproduced in the experiments of Mallik and Dasgupta (2012) (Fig. 9e) whose experimental melts had lower FeO^T than most OIBs. They proposed that a hotter mantle adiabat possibly in combination with an Fe-enriched source could explain the high Fe-contents of OIBs and this might also explain the high FeO^T of the Py1 melts. The unreacted eclogite melt used by Mallik and Dasgupta has very low K_2O and is therefore not representative of the RC basalts in this respect.

Dissolution and precipitation of clinopyroxene, orthopyroxene, garnet and olivine during melt–rock reaction processes cannot, however, be responsible for generating the different trace element patterns of the High and Low Nb/U groups since none of these minerals fractionate the most incompatible elements significantly (e.g. Kennedy et al., 1993; Jeffries et al., 1995; Johnson, 1998; Hill et al., 2011). Accessory phases in the eclogite such as rutile or ilmenite could fractionate Nb from U because high field strength elements such as Nb, Ta, Hf and Zr are far more compatible than U and Th but they cannot fractionate Ce from Pb or Ba from Th since these elements are all highly incompatible (Klemme et al., 2005, 2006). Therefore residual rutile during eclogite melting is not able to explain the different Ce/Pb and Ba/Th ratios (Fig. 7a) of the High and Low Nb/U groups.

During melt–rock reaction between the eclogite melt and the ambient peridotite, the melt would be expected to assimilate a part of the incompatible trace element budget of the peridotitic mantle through chromatographic processes and the trace element contents would be further modified when the eclogite melts are later mixed with peridotite melts formed at lower pressures. Mixing with depleted mantle-type trace element patterns would explain the higher Nb/U and Ce/Pb of the High Nb/U group as well as the lower La/Sm, Th/Nb, Th/La, K_2O/TiO_2 and Rb/Sr (Figs. 3, 6, 7 and 10). However, the higher Ba/Th of the High Nb/U basalts would require that the depleted mantle source had high Ba/Th unless the degree of melting of the depleted mantle was very low (1–2%) in which case the Ba/Th could be highly increased in the peridotite melts (Stracke and Bourdon, 2009). High Ba/Th is not found in South Atlantic N-MORB (Fig. 7) and it is not likely to be found in the lithospheric mantle below the Payenia region either (see Section 6.3). Moreover, metasomatism of South Atlantic N-MORB mantle or the lithospheric mantle by slab fluids cannot account for the high Ba since this would inevitably have led to decreased Ce/Pb and Nb/U as well.

OIBs from the same hot spot are often seen to have both enriched and depleted mantle sources distinct from the ambient MORB mantle

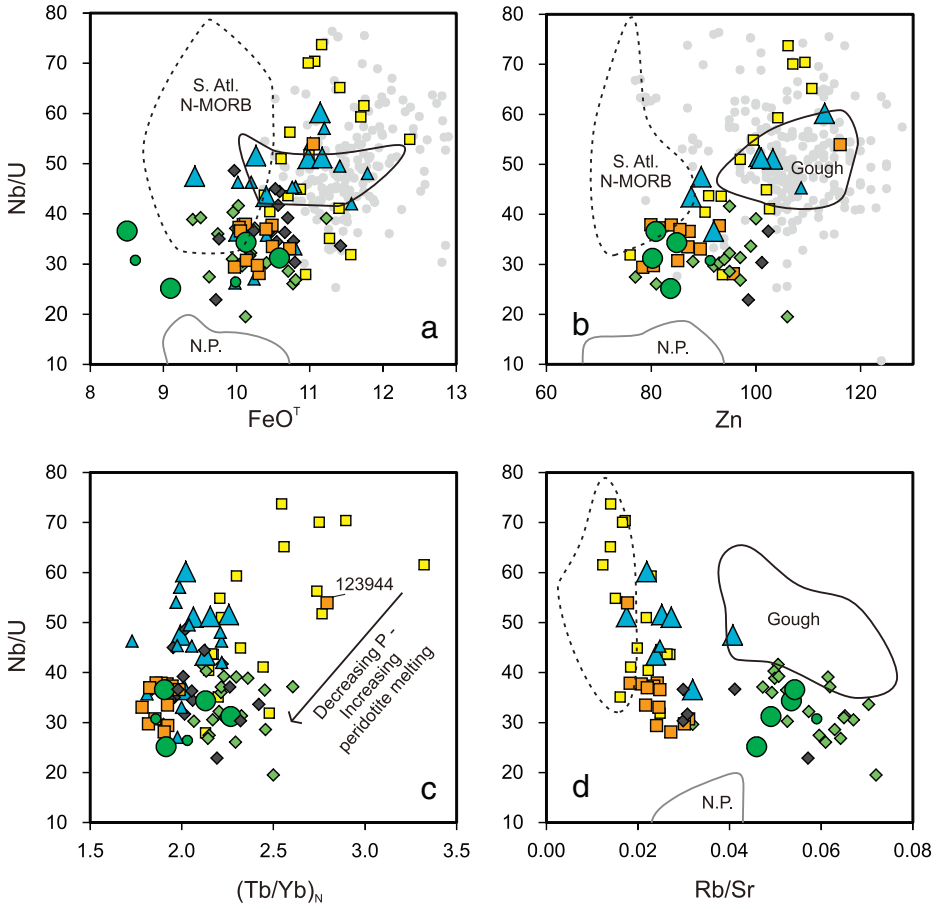

Fig. 10. a–d: Nb/U vs. FeO^T, Zn, $(Tb/Yb)_N$ (Normalisation values from McDonough and Sun (1995)) and Rb/Sr. Only the least contaminated samples with Mg# > 55 are plotted. The RC high Nb/U, Payún Matrú, Auca Mahuida and Matancilla basalts range from high Nb/U, FeO^T and Zn in the range of OIBs such as Hawaii and Gough to lower Nb/U, FeO^T and Zn similar to south Atlantic N-MORB. Symbols as in Fig. 9. References as in Figs. 2 and 3.

and they have been interpreted to represent different parts of a recycled oceanic lithosphere (e.g. Hofmann and Jochum, 1996; Abouchami and Hofmann, 1998; Chauvel and Hemond, 2000; Geldmacher and Hoernle, 2000). In the same way, the peridotite with which the eclogite melts reacted, could be depleted peridotite mantle from the same recycled lithosphere as the eclogite, for example the lithospheric mantle. If the oceanic lithosphere was recycled relatively recently, it could have an isotopic composition not so different from the eclogite. Thereby, the eclogite melts with high trace element contents could assimilate and mix with trace elements from the depleted peridotite without changing the isotopic composition and later be diluted by peridotite melts from the South Atlantic ambient mantle in the form of Pe1 melts.

Alternatively, the high and low Nb/U basalts have been formed from two different sources with identical isotopic composition. This could for example be from the lower and upper crustal parts of a recycled portion of oceanic crust, but it is unlikely that sources generating basalts with so different Rb/Sr (Fig. 10d) and Sm/Nd (not shown) would have the same Sr–Nd-isotopic composition. Generation of low Nb/U melts by re-melting of solidified basaltic melt or pyroxenitic cumulates of high Nb/U type composition in the lithospheric mantle would require no contamination of the Sr–Nd–Pb-isotope ratios from the surrounding lithospheric mantle and that either the fractional crystallisation or melting process involved a mineral assemblage which could fractionate the trace element patterns from high Nb/U to low Nb/U type patterns. Since neither amphibole, clinopyroxene nor ilmenite is alone capable of causing all of the observed trace element differences, it would have to be a multi-mineral assemblage. This is also the case if the trace element changes were formed by recent recrystallisation processes in the mantle source. However, by re-melting of solidified basaltic melt or pyroxenitic cumulates, the degree of melting should have been high in order to generate basaltic melts and this rules out the possible influence from minor exotic phases in the melting residual since they would have been melted out. The formation of the two trace element groups and the linkage between the major and trace element systematics remain presently unresolved. The model in Section 6.5.4 is based on the assumption that both high and low Nb/U magmas were generated from the same type of eclogite components in the mantle.

6.5.3. Low pressure peridotite melt addition

The mixing between the Py1-type melts and the low pressure Pe1 peridotite melts among the RC high Nb/U, Auca Mahuida, Matancilla and Payún Matrú basalts led to a decrease in the FeO^T and Ni contents of the melts as the amount of peridotite melt increased (Fig. 9e and f). Fig. 10a–c show that the lower FeO^T is accompanied by lower Nb/U, $(Tb/Yb)_N$ and lower Zn contents, in particular in the Payún Matrú basalts. The diagrams in Fig. 10 include the least contaminated samples with Mg# > 55 which have presumably only fractionated minor amounts of clinopyroxene. The Zn contents should therefore be close to the concentrations in the primary melts since Zn has a K_D(olivine) ~1 in contrast to Ni and Co which are both compatible in olivine (le Roux et al., 2011). The decreasing Nb/U is interpreted as a sign of an increasing input of peridotite melts with lower Nb/U and lower FeO^T and Zn similar to the peridotite derived South Atlantic N-MORB melts (le Roux et al., 2002). Peridotite lithologies typically have higher solidus temperatures than pyroxenites (Kogiso et al., 2004) and therefore peridotite mantle would start melting higher in the melting column than any entrained bodies of eclogite. The larger peridotite component in the Payún Matrú basalts could therefore be related to a thinner lithosphere as is also suggested by the low $(Tb/Yb)_N$ of the young Payún Matrú rocks which indicates low amounts of residual garnet in the mantle source and hence low pressure of melt formation (Søager et al., 2013). The significantly higher $(Tb/Yb)_N$ of the Matancilla basalts and the older Payún Matrú lavas erupted from the same area (of which only sample 123944 is plotted in Fig. 10) thus implies a thinning of the lithosphere before the formation of the young Payún Matrú complex. If the Pe1 peridotite melts are produced by melting of the ambient South Atlantic upper mantle, then the generally lower Nb/U, Ce/Pb and $^{143}Nd/^{144}Nd$ and higher Ba/Nb, Th/Nb and $^{87}Sr/^{86}Sr$ of the young Payún Matrú basalts relative to the Matancilla, RC and South Atlantic N-MORB basalts (see also Fig. 6) could reflect melting of a weakly metasomatised mantle wedge above the subducting slab in the western Payenia region after the shallow subduction period during the late Miocene to Pleistocene.

6.5.4. Possible mantle temperature differences

If the major element characteristics of the low Nb/U melts reflect eclogite melts that reacted less with the peridotitic mantle during ascent than the high Nb/U melts, this could suggest that they ascended through channels that were insulated by previous eclogite melts (Mallik and Dasgupta, 2012) or/and that they formed in lower temperature mantle which melted at shallower levels. This would give the melts a shorter path where they could react with the peridotite before melt segregation and eruption (Fig. 11). A thicker lithosphere could possibly give the same effect because it shortens the melting column, but since high and low Nb/U lavas occur in the same volcanoes they must be assumed to have formed under the same lithospheric thickness which is also supported by the similar range of $(Tb/Yb)_N$ in the two groups (Fig. 10c). The apparent lack of mixing between low Nb/U-type melts and Pe1 peridotite melts could indicate that the temperature was too low to melt the peridotite in these instances. In contrast, the mixing with peridotite melts that apparently occurred in most high Nb/U type melts suggests a somewhat elevated mantle temperature because the peridotite is not expected to melt at normal mantle temperatures. This temperature difference is supported by the REE melting model from Søager et al. (2013) where lower $(La/Sm)_N$ at a given $(Tb/Yb)_N$ in the RC high Nb/U, Payún Matrú, Auca Mahuida and Matancilla basalts indicates higher initial melting pressures and degrees of melting and thus higher mantle potential temperatures relative to what is indicated for the low Nb/U and North Patagonian basalts (see Supplementary Fig. A2).

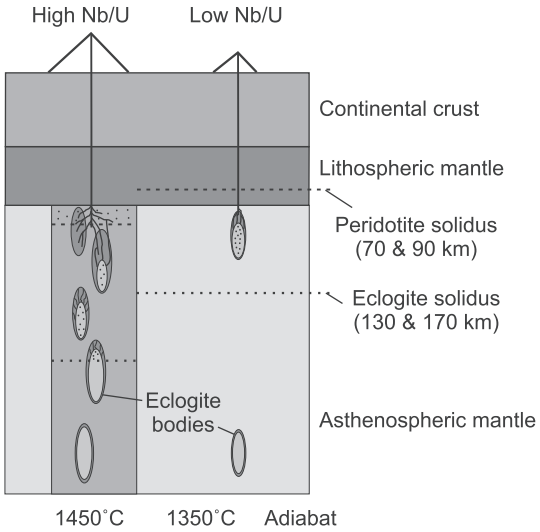

Fig. 11. A schematic model for the formation of the major element variations in the high and low Nb/U basalts. Black dots mark the zones of melting. The model shows two scenarios: A 1350 °C mantle adiabat where the eclogite bodies begin to melt ~130 km depth, assuming a solidus temperature similar to the NAM-7 MORB basalt (Yasuda et al., 1994), and the peridotite solidus pressure is not reached beneath the lithosphere–asthenosphere boundary (LAB). The second scenario is for a 1450 °C mantle adiabat where the eclogite bodies begin to melt ~170 km depth and the peridotite solidus is transgressed just below the LAB. Here, the eclogite melts have longer paths along which to react with the surrounding peridotite before melt segregation at the LAB and they will be mixed with the peridotite melts. At depth, the eclogite bodies are shown with a rim representing a zone of solid-state reaction between eclogite and peridotite (Mallik and Dasgupta, 2012). The model is partly adopted from Mallik and Dasgupta (2012).

7. Conclusions

The southern Payenia basalts have compositions which are isotopically and elementally similar to basalts from NW Patagonia but distinct from the south Patagonian basalts. Although the Payenia source is found in the areas of earlier shallow subduction, its composition is of EM1 OIB-type and is unrelated to the subduction environment. Furthermore, its composition is distinct from that of the local lithospheric mantle which is therefore an unlikely source. The RC (Río Colorado) lavas fall in two groups with different trace element patterns but the same range of isotopic compositions, here called the high and low Nb/U groups. The trace element patterns can be explained by mixing between recycled MORB and recycled lower continental crust.

The fractionation corrected major element contents suggest that the low Nb/U and high Nb/U basalts can have been formed from eclogite melts which interacted with peridotite to a low and high degree, respectively. The high Nb/U melts were in most cases mixed with peridotite melts formed at lower pressures, in particular in the Payún Matrú area. This difference between the groups may be related to an elevated mantle temperature in the areas where high Nb/U basalts dominate: Payún Matrú, Auca Mahuida and the Río Colorado region and in the early Miocene Matancilla basalts. The low Nb/U melts were possibly formed in lower temperature mantle where the eclogite melted at a shallower depth and equilibrated less with the surrounding peridotite. Alternatively, these melts may have ascended through channels that were insulated by previous eclogite melts and therefore experienced less interaction with the surrounding peridotitic mantle.

Supplementary data to this article can be found online at http://dx.doi.org/10.1016/j.chemgeo.2013.10.024.

Acknowledgements

We thank Andreas Stracke and one anonymous reviewer as well as the editor Laurie Reisberg for the excellent comments and considerable effort in the review process. We are grateful for the constructive criticism from Eduardo Llambías and Gustavo Bertotto. Jonas Gudnason, Frederik Brandt and Charlotte Thorup Dyhr are thanked for their assistance and for many good discussions. We greatly acknowledge the support to P.M. Holm from the Danish Research Council for Nature and Universe grant no. 272-07-0514 and the Carlsberg Foundation grant no. 2010_01_0833 and the Faculty of Science, University of Copenhagen, for a Ph.D. stipend to NS.

References

Abouchami, W., Hofmann, A.W., 1998. Triple-spike Pb isotope data on Hawaii Scientific Drilling Project (HSDP) lavas: the roles of upper mantle and lower oceanic crust. Mineral. Mag. 62A (1–3), 5–6.

Baker, J., Peate, D., Waight, T., Meyzen, C., 2004. Pb isotopic analysis of standards and samples using a ^{207}Pb–^{204}Pb and thallium to correct for mass bias with a double-focusing MC-ICP-MS. Chem. Geol. 211, 275–303.

Balta, J.B., Asimow, P.D., Mosenfelder, J.L., 2011. Hydrous low-carbon melting of garnet peridotite. J. Pet. 52 (11), 2079–2105.

Barnes, S.J., Roeder, P.L., 2001. The range of spinel compositions in terrestrial mafic and ultramafic rocks. J. Pet. 42 (12), 2279–2302.

Bermudez, A., Delpino, D., Frey, F., Saal, A., 1993. Los basaltos de retroarco extraandinos, in: Ramos, V.A. (Ed.), Geología y Recursos Naturales de Mendoza. Relatorio I (13), 161–172.

Bertotto, G.W., 2000. Cerro Agua Poca, un cono basáltico cuaternario portador de xenolitos ultramáficos, en el oeste de la provincia de La Pampa, Argentina. Rev. Asoc. Geol. Argent. 55 (1/2), 59–71.

Bertotto, G.W., 2003. Evolución geológica y petrológica de los conos basálticos cenozoicos portadores de xenolitos ultramáficos del margen oriental de la Provincia basáltica Andino-Cuyana, provincias de La Pampa y Mendoza. (Unpublished PhD Thesis) Universidad Nacional de La Plata, La Plata 196.

Bertotto, G.W., Orihashi, Y., Nagao, K., Motoki, A., 2006. New K–Ar ages on retroarc basalts of Mendoza-La Pampa. Abstract. Second scientific meeting of the ICES, Buenos Aires. Actas CD.

Bertotto, G.W., Cingolani, C.A., Bjerg, E.A., 2009. Geochemical variations in Cenozoic back-arc basalts at the border of La Pampa and Mendoza provinces, Argentina. J. S. Am. Earth Sci. 28, 360–373.

Bjerg, E.A., Ntaflos, T., Thöni, M., Aliani, P., Labudia, C.H., 2009. Heterogeneous lithospheric mantle beneath northern Patagonia: evidence from Prahuaniyeu garnet- and spinel-peridotites. J. Pet. 50 (7), 1267–1298.

Chauvel, C., Hemond, C., 2000. Meltin of a complete section of recycled oceanic crust: trace element and Pb isotopic evidence from Iceland. Geochem. Geophys. Geosyst. 1, 1.

Class, C., le Roex, A.P., 2011. South Atlantic DUPAL anomaly—dynamic and compositional evidence against a recent shallow origin. Earth Planet. Sci. Lett. 305, 92–102.

Conceição, R.V., Mallmann, G., Koester, E., Schilling, M., Bertotto, G.W., Rodriguez-Vargas, A., 2005. Andean subduction-related mantle xenoliths: isotopic evidence of Sr–Nd decoupling during metasomatism. Lithos 82, 273–287.

Dantas, C., Grégoire, M., Koester, E., Conceicão, R.E., Rieck Jr., N., 2009. The lherzolite–websterite xenolith suite from Northern Patagonia (Argentina): evidence of mantle–melt reaction processes. Lithos 107, 107–120.

Dasgupta, R., Jackson, M.G., Lee, C.-T.A., 2010. Major element chemistry of ocean island basalts—conditions of mantle melting and heterogeneity of mantle source. Earth Planet. Sci. Lett. 289, 377–392.

Douglass, J., Schilling, J.-G., 1999. Plume–ridge interactions of the Discovery and Shona mantle plumes with the southern Mid-Atlantic Ridge (40°–55°S). J. Geophys. Res. 104 (B2), 2941–2962.

Dungan, M.A., Wulff, A., Thompson, R., 2001. Eruptive stratigraphy of the Tatara-San Pedro complex, 36°S, Southern Volcanic Zone, Chilean Andes: reconstruction method and implications for magma evolution at long-lived arc volcanic centres. J. Petrol. 42, 555–626.

Dyhr, C.T., Holm, P.M., Llambías, E.J., Scherstén, A., 2013a. Subduction controls on Miocene backarc lavas from Sierra de Huantraico and La Matancilla and new $^{40}Ar/^{39}Ar$ dating from the Mendoza region, Argentina. Lithos 179, 67–83.

Dyhr, C.T., Holm, P.M., Llambías, E.J., 2013b. Geochemical constraints on the relationship between the Miocene–Pliocene volcanism and tectonics in the Palaoco and Fortunoso volcanic fields, Mendoza Region, Argentina: new insights from $^{40}Ar/^{39}Ar$ dating, Sr–Nd–Pb isotopes and trace elements. J. Volcanol. Geotherm. Res. 266, 50–68.

Elkins, L.J., Gaetani, G.A., Sims, K.W.W., 2008. Partitioning of U and Th during garnet pyroxenite partial melting: constraints on the source of alkaline ocean island basalts. Earth Planet. Sci. Lett. 265 (1–2), 270–286.

Escrig, S., Schiano, P., Schilling, J.-G., Allègre, C., 2005. Rhenium–osmium systematics in MORB from the Southern mid-Atlantic Ridge (40°–50°S). Earth Planet. Sci. Lett. 235, 528–548.

Espinoza, F., Morata, D., Pelleter, E., Maury, R.C., Suarez, M., Lagabrielle, Y., Polve, M., Bellon, H., Cotten, J., de la Cruz, R., Guivel, C., 2005. Petrogenesis of the Eocene and Mio-Pliocene alkaline basaltic magmatism in Meseta Chile Chico, southern Patagonia, Chile; evidence for the participation of two slab windows. Lithos 82 (3–4), 315–343.

Folguera, A., Naranjo, J.A., Orihashi, Y., Sumino, H., Nagao, K., Polanco, E., Ramos, V.A., 2009. Retroarc volcanism in the northern San Rafael block (34º–35º30′S), southern Central Andes: occurrence, age and tectonic setting. J. Volcanol. Geotherm. Res. 186, 169–185.

Fontignie, D., Schilling, J.-G., 1996. Mantle heterogeneities beneath the South Atlantic: a Nd–Sr–Pb isotope study along the mid-Atlantic ridge (3°S–46°S). Earth Planet. Sci. Lett. 142, 209–221.

Frey, F.A., Garcia, M.O., Roden, M.F., 1994. Geochemical characteristics of Koolau volcano: implications of intershield geochemical differences among Hawaiian volcanoes. Geochim. Cosmochim. Acta 58 (5), 1441–1462.

Gaetani, G.A., Grove, T.L., 1998. The influence of water on melting of mantle peridotite. Contrib. Mineral. Petrol. 131, 323–346.

Geldmacher, J., Hoernle, K., 2000. The 72 Ma geochemical evolution of the Madeira hotspot (eastern North Atlantic): recycling of Paleozoic (≤500 Ma) oceanic lithosphere. Earth Planet. Sci. Lett. 183, 73–92.

Germa, A., Quidelleur, X., Gillot, P.Y., Tchilinguirian, P., 2010. Volcanic evolution of the backarc Pleistocene Payún Matrú volcanic field (Argentina). J. S. Am. Earth Sci. 29, 717–730.

Gibson, S.A., Thompson, R.N., Day, J.A., Humphris, S.E., Dickin, A.P., 2005. Melt-generation processes associated with the Tristan mantel plume: constraints on the origin of EM1. Earth Planet. Sci. Lett. 237, 744–767.

Gorring, M.L., Kay, S.M., 2001. Mantle processes and sources of Neogene slab window magmas from southern Patagonia, Argentina. J. Petrol. 42 (6), 1067–1094.

Gudnason, J., Holm, P.M., Søager, N., Llambías, E.J., 2012. Geochronology of the late Pliocene to Recent volcanic activity in the Payenia back-arc volcanic province, Mendoza, Argentina. J. S. Am. Earth Sci. 37, 191–201.

Gurenko, A.A., Sobolev, A.V., Hoernle, K.A., Hauff, F., Schmincke, H.-U., 2009. Enriched, HIMU-type peridotite and depleted recycled pyroxenite in the Canary plume: a mixed-up mantle. Earth Planet. Sci. Lett. 277, 514–524.

Gurenko, A.A., Hoernle, K.A., Sobolev, A.V., Hauff, F., Schmincke, H.-U., 2010. Source components of the Gran Canaria (Canary Islands) shield stage magmas: evidence from olivine composition and Sr–Nd–Pb isotopes. Contrib. Mineral. Petrol. 159, 689–702.

Hanan, B.B., Blichert-Toft, J., Pyle, D.G., Christie, D.M., 2004. Contrasting origins of the upper mantle revealed by hafnium and lead isotopes from the Southeast Indian Ridge. Nature 432, 91–94.

Hart, S.R., 1984. The Dupal anomaly: a large-scale isotope anomaly in the southern hemisphere mantle. Nature 309, 753–757.

Hart, B.T., Davies, S.H.R., 1978. Nickel partitioning between olivine and silicate melt. Earth Planet. Sci. Lett. 40, 203–219.

Hawkesworth, C.J., Mantovani, M.S.M., Taylor, P.N., Palacz, Z., 1986. Evidence from the Parana of south Brazil for a continental contribution to Dupal basalts. Nature 322, 356–359.

Hernando, I.R., Llambías, E.J., González, P.D., Sato, K., 2012. Volcanic stratigraphy and evidence of magma mixing in the Quarternary Payun Matru volcano, andean backarc in western Argentina. Andean Geol. 39 (1), 158–179.

Herzberg, C., 2006. Petrology and thermal structure of the Hawaiian plume from Mauna Kea volcano. Nature 444, 605–609.
Herzberg, C., 2011. Identification of source lithology in the Hawaiian and Canary Islands: implications for origins. J. Petrol. 52 (1), 113–146.
Herzberg, C., Asimov, P.D., 2008. Petrology of some oceanic island basalts: PRIMELT2.XLS software for primary magma calculation. Geochem. Geophys. Geosyst. 9, 9. http://dx.doi.org/10.1029/2008GC002057.
Hill, E., Blundy, J.D., Wood, B.J., 2011. Clinopyroxene-melt trace element partitioning and the development of a predictive model for HFSE and Sc. Contrib. Mineral. Petrol. 161, 423–438.
Hirose, K., Kushiro, I., 1993. Partial melting of dry peridotites at high pressures: determination of compositions of melts segregated from peridotite using aggregates of diamond. Earth Planet. Sci. Lett. 114, 477–489.
Hirschmann, M.M., Ghiorso, M.S., Stolper, E.M., 1999. Calculation of peridotite partial melting from thermodynamic models of minerals and melts. II. Isobaric variations in melts near the solidus and owing to variable source composition. J. Petrol. 40 (2), 297–313.
Hofmann, A.W., Jochum, K.P., 1996. Source characteristics derived from very incompatible trace elements in Mauna Loa and Mauna Kea basalts, Hawaii Scientific Drilling Project. J. Geophys. Res. 101 (B5), 11,831–11,839.
Horn, I., Foley, S.F., Jackson, S.E., Jenner, G.A., 1994. Experimentally determined partitioning of high field strength- and selected transition elements between spinel and basaltic melt. Chem. Geol. 117, 193–218.
Jackson, M.G., Dasgupta, R., 2008. Compositions of HIMU, EM1, and EM2 from global trends between radiogenic isotopes and major elements in ocean island basalts. Earth Planet. Sci. Lett. 276, 175–186.
Jacques, G., Hoernle, K., Gill, J., Hauff, F., Wehrmann, H., Garbe-Schönberg, D., van den Bogaard, P., Bindeman, I., Lara, L.E., 2013. Across-arc geochemical variations in the Southern Volcanic Zone, Chile (34.5–38.0°S): constraints on mantle wedge and slab input compositions. Geochim. Cosmochim. Acta 123, 218–243. http://dx.doi.org/10.1016/j.gca.2013.05.016.
Jeffries, T.E., Perkins, W.T., Pearce, N.J.G., 1995. Measurements of trace elements in basalts and their phenocrysts by laser probe microanalysis inductively coupled plasma mass spectrometry (LPMA-ICP-MS). Chem. Geol. 121, 131–144.
Johnson, K.T.M., 1998. Experimental determinations of partition coefficients for rare earth and high-field-strength elements between clinopyroxene, garnet, and basaltic melt at high pressures. Contrib. Mineral. Petrol. 133, 60–68.
Kamenetsky, V.S., Maas, R., Sushcevskaya, N.M., Norman, M.D., Cartwright, I., Peyve, A.A., 2001. Remnants of Gondwanan continental lithosphere in oceanic upper mantle: evidence from the South Atlantic Ridge. Geology 29, 243–246.
Kay, S.M., Copeland, P., 2006. Early to middle Miocene backarc magmas of the Neuquén Basin: geochemical consequences of slab shallowing and the westward drift of South America. Late Cretaceous to Recent magmatism and tectonism of the Southern Andean margin at the latitude of the Neuquen basin (36–39°S). In: Kay, S.M., Ramos, V.A. (Eds.), Geol. Soc. Am., Spec. Pap., 407, pp. 185–213.
Kay, S.M., Gorring, M., Ramos, V.A., 2004. Magmatic sources, setting, and causes of Eocene to Recent Patagonian plateau magmatism (36 degrees S to 52 degrees S latitude). Rev. Asoc. Geol. Argent. 59 (4), 556–568.
Kay, S.M., Burns, M., Copeland, P., Mancilla, O., 2006a. Upper Cretaceous to Holocene magmatism over the Neuquén basin: evidence for transient shallowing of the subduction zone under the Neuquén Andes (36°S to 38°S latitude). Late Cretaceous to Recent magmatism and tectonism of the Southern Andean margin at the latitude of the Neuquen basin (36–39°S). In: Kay, S.M., Ramos, V.A. (Eds.), Geol. Soc. Am., Spec. Pap., 407, pp. 19–60.
Kay, S.M., Copeland, P., Mancilla, O., 2006b. Evolution of the late Miocene Chachahuén volcanic complex at 37 °S over a transient shallow subduction zone under the Neuquén Andes. Late Cretaceous to Recent magmatism and tectonism of the Southern Andean margin at the latitude of the Neuquen basin (36–39°S). In: Kay, S.M., Ramos, V.A. (Eds.), Geol. Soc. Am., Spec. Pap., 407, pp. 215–246.
Kay, S.M., Ardolino, A.A., Gorring, M.L., Ramos, V.A., 2007. The Somuncura large igneous province in Patagonia: interaction of a mantle thermal anomaly with a subducting slab. J. Petrol. 48 (1), 43–77.
Kay, S.M., Jones, H.A., Kay, R.W., 2013. Origin of Tertiary to Recent EM- and subduction-like chemical and isotopic signatures in Auca Mahuida region (37–38°) and other Patagonian plateau lavas. Contrib. Mineral. Petrol. 166 (1), 165–192.
Kendrick, E., Bevis, M., Smalley Jr., R., Brooks, B., Barriga Vargas, R., Lauría, E., Fortes, L.P.S., 2003. The Nazca-South America Euler vector and its rate of change. J. S. Am. Earth Sci. 16, 125–131.
Kennedy, A.K., Lofgren, G.E., Wasserburg, G.J., 1993. An experimental study of trace element partitioning between olivine, orthopyroxene and melt in chondrules—equilibrium values and kinetic effects. Earth Planet. Sci. Lett. 115, 177–195.
Klemme, S., Prowatke, S., Hametner, K., Günther, D., 2005. Partitioning of trace elements between rutile and silicate melts: implications for subduction zones. Geochim. Cosmochim. Acta 69 (9), 2361–2371.
Klemme, S., Günther, D., Hametner, K., Prowatke, S., Zack, T., 2006. The partitioning of trace elements between ilmenite, ulvospinel, armalcolite and silicate melts with implications for the early differentiation of the moon. Chem. Geol. 234, 251–263.
Kogiso, T., Hirose, K., Takahashi, E., 1998. Melting experiments on homogeneous mixtures of peridotite and basalt: application to the genesis of ocean island basalts. Earth Planet. Sci. Lett. 162, 45–61.
Kogiso, T., Hirschmann, M.M., Pertermann, M., 2004. High-pressure partial melting of mafic lithologies in the mantle. J. Petrol. 45 (12), 2407–2422.
Le Roex, A.P., 1985. Geochemistry, mineralogy and magmatic evolution of the basaltic and trachytic lavas from Gough Island, South Atlantic. J. Petrol. 26, 149–186.
Le Roex, A.P., Cliff, R.A., Adair, J.I., 1990. Tristan da Cunha, South Atlantic: geochemistry and petrogenesis of a basanite–phonolite lava series. J. Petrol. 31, 779–812.
Le Roex, A., Class, C., O'Connor, J., Jokat, W., 2010. Shona and discovery aseismic ridge systems, South Atlantic; trace element evidence for enriched mantle sources. J. Pet. 51 (10), 2089–2120.
Le Roux, P.J., le Roex, A.P., Schilling, J.-G., Shimizu, N., Perkins, W.W., Pearce, N.J.G., 2002. Mantle heterogeneity beneath the southern Mid-Atlantic ridge: trace element evidence for contamination of ambient asthenospheric mantle. Earth Planet. Sci. Lett. 203, 479–498.
Le Roux, V., Dasgupta, R., Lee, C.-T.A., 2011. Mineralogical heterogeneities in the Earth's mantle: Constraints from Mn, Co, Ni and Zn partitioning during partial melting. Earth Planet. Sci. Lett. 307, 395–408.
Litvak, V.D., Folguera, A., Ramos, V.A., 2008. Determination of an arc-related signature in late Miocene volcanic rocks over the San Rafael block, Southern Central Andes (34°30–37°S), Argentina: the Payenia shallow subduction zone. 7th Int. Symp. And. Geodyn., Nice, ext. abstracts, pp. 289–291.
Lopez-Escobar, L., Parada, M.A., Hickey-Vargas, R., Frey, F.A., Kempton, P.D., Moreno-Roa, H., 1995. Calbuco volcano and minor eruptive centers distributed along the Liquiñe-Ofqui fault zone, Chile (41°–42°S): contrasting origin of andesitic and basaltic magma in the Southern Volcanic Zone of the Andes. Contrib. Mineral. Petrol. 119, 345–361.
Lucassen, F., Escayola, M., Romer, R.L., Viramonte, J., Koch, K., Franz, G., 2002. Isotopic composition of Late Mesozoic basic and ultrabasic rocks from the Andes (23–32°S)—implications for the Andean mantle. Contrib. Mineral. Petrol. 143, 336–349.
Lucassen, F., Franz, G., Viramonte, J., Romer, R.L., Dulski, P., Lang, A., 2005. The late Cretaceous lithospheric mantle beneath the Central Andes: evidence from phase equilibria and composition of mantle xenoliths. Lithos 82, 379–406.
Mallik, A., Dasgupta, R., 2012. Reaction between MORB-eclogite derived melts and fertile peridotite and generation of ocean island basalts. Earth Planet. Sci. Lett. 329–330, 97–108.
Massaferro, G.I., Haller, M.J., D'Orazio, M., Alric, V.I., 2006. Sub-recent volcanism in Northern Patagonia: a tectonomagmatic approach. J. Volcanol. Geotherm. Res. 155, 227–243.
McDonough, W.F., Sun, S.S., 1995. The composition of the Earth. Chem. Geol. 120 (3–4), 223–253.
McKenzie, D., O'Nions, R.K., 1995. The source region of ocean island basalts. J. Pet. 36, 133–159.
Melchor, R., Casadío, S., 1999. Hoja geológica 3766-III La Reforma, provincia de la Pampa. Secretaría de Minería de la Nación, SEGEMAR, Boletín, 295, p. 63 (Buenos Aires).
Meyzen, C.M., Ludden, J.N., Humler, E., Luais, B., Toplis, M.J., Mével, C., Storey, M., 2005. New insights into the origin and distribution of the DUPAL isotope anomaly in the Indian Ocean mantle from MORB of the Southwest Indian Ridge. Geochem. Geophys. Geosyst. 6. http://dx.doi.org/10.1029/2005GC000979.
Meyzen, C.M., Blichert-Toft, J., Ludden, J.N., Humler, E., Mével, C., Albarède, F., 2007. Isotopic portrayal of the Earth's upper mantle flow field. Nature 447, 1069–1073.
Milner, S.C., Le Roex, A.P., 1996. Isotope characteristics of the Okenyenya igneous complex, northwestern Namibia: constraints on the composition of the early Tristan plume and the origin of the EM1 mantle component. Earth Planet. Sci. Lett. 141, 277–291.
Muñoz, J.B., Stern, C.R., 1988. The Quaternary volcanic belt of the southern continental margin of South America: transverse structural and petrochemical variations across the segment between 38°S and 39°S. J. S. Am. Earth Sci. 1 (2), 147–161.
Núñez, E., 1976. Descripción geológica de la Hoja 31e Chical-Có, provincias de Mendoza y La Pampa. (Informe Inédito) Servicio Nacional Geológico Minero, Buenos Aires (92 pp.).
Pasquaré, G., Bistacchi, A., Francalanci, L., Bertotto, G.W., Boari, E., Massironi, M., Rossotti, A., 2008. Very long pahoehoe inflated basaltic lava flows in the Payenia volcanic province (Mendoza and La Pampa, Argentina). Rev. Asoc. Geol. Argentina 63 (1), 131–149.
Pertermann, M., Hirschmann, M.M., 2003. Anhydrous partial melting experiments on MORB-like eclogite: phase relations, phase compositions and mineral–melt partitioning of major elements at 2–3 GPa. J. Petrol. 44, 2173–2201.
Pertermann, M., Hirschmann, M.M., Hametner, K., Günther, D., Schmidt, M.W., 2004. Experimental determination of trace element partitioning between garnet and silica-rich liquid during anhydrous partial melting of MORB-like eclogite. Geochem. Geophys. Geosyst. 5, 5. http://dx.doi.org/10.1029/2003GC000638.
Ramos, V.A., 2010. The Grenville-age basement of the Andes. J. S. Am. Earth Sci. 29, 77–91.
Regelous, M., Niu, Y., Abouchami, W., Castillo, P.R., 2009. Shallow origin for South Atlantic Dupal Anomali from lower continental crust: geochemical evidence from the Mid-Atlantic Ridge at 26°S. Lithos 112, 57–72.
Ren, Z.-Y., Hanuy, T., Miyazaki, T., Chang, Q., Kawabata, H., Takahashi, T., Hirahara, Y., Tatsumi, Y., 2009. Geochemical differences of the Hawaiian shield lavas: implications for melting process in the heterogeneous Hawaiian plume. J. Petrol. 50 (8), 1553–1573.
Righter, K., Leeman, W.P., Hervig, R.L., 2006. Partitioning of Ni, Co and V between spinel-structured oxides and silicate melts: importance of spinel composition. Chem. Geol. 227, 1–25.
Rosello, E.A., Cobbold, P.R., Diraison, M., Arnaud, N., 2002. Auca Mahuida (Neuquén Basin, Argentina): a Quarternary shield volcano on a hydro-carbon producing substrate. 5° Int. Symp. Andean Geodyn., Toulouse, ext. abstracts, pp. 549–552.
Rudnick, R.L., Gao, S., 2003. Composition of the continental crust. In: Carlson, R.W., Holland, H.D., Turekian, K.K. (Eds.), Treatise on Geochemistry: The Crust. Elsevier, pp. 1–64.
Salters, V.J.M., Longhi, J.E., 1999. Trace element partitioning during the initial stages of melting beneath mid-ocean ridges. Earth Planet. Sci. Lett. 166, 15–30.
Salters, V.J.M., Stracke, A., 2004. Composition of the depleted mantle. Geochem. Geophys. Geosyst. 5, Q055004. http://dx.doi.org/10.1029/2003GC000597.
Skulski, T., Minarik, W., Watson, E.B., 1994. High-pressure experimental trace element partitioning between clinopyroxene and basaltic melts. Chem. Geol. 117, 127–147.

Søager, N., Holm, P.M., Llambías, E.J., 2013. Payenia volcanic province, southern Mendoza, Argentina: OIB mantle upwelling in a backarc environment. Chem. Geol. 349–350, 36–53.

Sobolev, A.V., Hofmann, A.W., Sobolev, S.W., Nikogosian, I.G., 2005. An olivine-free mantle source of Hawaiian shield basalts. Nature 434, 590–597.

Sobolev, A.V., Hofmann, A.W., Kuzmin, D.V., Yaxley, G.M., Arndt, N.A., Chung, S.-L., Danyushevsky, L.V., Elliott, T., Frey, F.A., Garcia, M.O., Gurenko, A.A., Kamenetsky, V.S., Kerr, A.C., Krivolutskaya, N.A., Matvienkov, V.V., Nikogosian, I.K., Rocholl, A., Sigurdsson, I.A., Sushchevskaya, N.M., Teklay, M., 2007. The amount of recycled crust in sources of mantle derived melts. Science 316, 412–417.

Spandler, C., Yaxley, G., Green, D.H., Rosenthal, A., 2008. Phase relations and melting of anhydrous K-bearing eclogite from 1200 to 1600 °C and 3 to 5 GPa. J. Petrol. 49 (4), 771–795.

Stern, C.R., Frey, F.A., Futa, K., Zartman, R.E., Peng, Z., Kyser, K.T., 1990. Trace element and Sr, Nd, Pb, and O isotopic composition of Pliocene and Quaternary alkali basalts of the Patagonian Plateau lavas of southernmost South America. Contrib. Mineral. Petrol. 104, 294–308.

Stracke, A., Bourdon, B., 2009. The importance of melt extraction for tracing mantle heterogeneity. Geochim. Cosmochim. Acta 73, 218–238.

Thirlwall, M.F., 2000. Inter-laboratory and other errors in Pb isotope analyses investigated using a ^{207}Pb–^{204}Pb double spike. Chem. Geol. 163, 299–322.

Varekamp, J.C., Hesse, A., Mandeville, C.W., 2010. Back-arc basalts from the Loncopue graben (Province of Neuquén, Argentina). J. Volcanol. Geotherm. Res. 197 (1–4), 313–328.

Walter, M.J., 1998. Melting of garnet peridotite and the origin of komatiite and depleted lithosphere. J. Petrol. 39 (1), 29–60.

Wang, Z., Gaetani, G.A., 2008. Partitioning of Ni between olivine and silicious eclogite partial melt: experimental constraints on the mantle source of Hawaiian basalts. Contrib. Mineral. Petrol. 156, 661–678.

Willbold, M., Stracke, A., 2006. Trace element composition of mantle end-members: implications for recycling of oceanic and upper and lower continental crust. Geochem. Geophys. Geosyst. 7, 4. http://dx.doi.org/10.1029/2005GC001005.

Willbold, M., Stracke, A., 2010. Formation of enriched mantle components by recycling of upper and lower continental crust. Chem. Geol. 276, 188–197.

Workman, R.K., Hart, S.R., 2005. Major and trace element composition of the depleted mantle. Earth Planet. Sci. Lett. 231, 53–72.

Yasuda, A., Fujii, T., Kurita, K., 1994. Melting phase relations of an anhydrous mid-ocean ridge basalt from 3 to 20 GPa: implications for the behaviour of subducted oceanic crust in the mantle. J. Geophys. Res. 99 (B5), 9401–9414.

Yaxley, G.M., Green, D.H., 1998. Reactions between eclogite and peridotite; mantle refertilisation by subduction of oceanic crust. Schweiz. Mineral. Petrogr. Mitt. 78 (2), 243–255.

Zindler, A., Hart, S.R., 1986. Chemical geodynamics. Annu. Rev. Earth Planet. Sci. 14, 493–571.